Heat transfer and thermally induced stresses in window glass coated with optically active nano-particles

A thesis presented for the degree of
Masters in Engineering

By

Humayer Ahmed Chowdhury

Institute of Nanoscale Technology
Faculty of Engineering
University of Technology, Sydney

May 2007

Declaration of original authorship

UNIVERSITY OF TECHNOLOGY SYDNEY

I certify that the work in this thesis has not previously been submitted for a degree nor has it been submitted as part of requirements for a degree except as fully acknowledged within the text.

I also certify that I am the primary and original author of this thesis, and any help I have received in my research work and its preparation has been acknowledged. In addition, I certify that all literature sources are cited and listed in the references of this thesis.

Production Note:
Signature removed prior to publication.

19/6/07

Humayer Ahmed CHOWDHURY   Date

Acknowledgements

Table of contents

List of Figures

List of Tables

Symbol Index - Nomenclature

English Letters	
A	Area of the glass, m^2
c_p	Specific heat
$D_{r,\theta}$	Diffusely emitted radiation as a function of distance, r and angle, θ
$D_{0,0}$	Surface intensity of radiation reflected perpendicularly from glass surface
E	Modulus of elasticity (Young Modulus)
E_λ	Spectral irradiance of the light source, $W.m^{-2}.nm^{-1}$, as $f(\lambda)$
F	Proportion of incident radiant energy transferred to the interior of the glass
Gr_L	Grashof number
h	Convective heat transfer coefficient, $W.m^{-2}.K^{-1}$
I_λ	Maximum specular reflectance
k	Thermal conductivity $W.m^{-1}.K^{-1}$
K_c	Stress intensity
l_0	Length at 273K
l_t	Length at temperature t
l	Mode of the resonance (l=1 produces a dipole resonance, l=2 a quadrupole resonance, l=3 a octupole resonance)
L	Height of the glass pane, m
m	Parameter accounting for decrease in $D_{r,\theta}$ as $f(r)$
n	Specular reflection exponent in Phong's Law
Nu_L	Nusselt number
Pr	Prandtl number
q	Heat transfer through or from glass surface, W
q_c	Convected heat energy
q_i	Incident heat energy
q_r	Heat energy radiated
Ra	Rayleigh number

R_{sol}	Proportion of the total solar irradiance that is reflected
T_o	Outside temperature
T_i	Inside temperature
T_{air}	Temperature of laboratory air, K
T_f	Film temperature K
T_s	Temperature of the glass surface, K
T_{vis}	Proportion of visible spectrum that is directly transmitted by glass
T_{sol}	Proportion of the total solar irradiance that is transmitted
T_λ	Total spectral transmissivity of the glass, as $f(\lambda)$
V_λ	Photo-optic luminous efficiency function of the human eye, as $f(\lambda)$
x	Ratio of the inner and outer radii of a nano-shell particle
Greek Symbols	
α	Thermal expansion co-efficient 1/°C
β	Volumetric coefficient of thermal expansion 1/°C
ϵ	Emissivity
γ	Angular deviation from specular reflection
v	Poisson's ratio
ρ	Density kg/m^3
$\epsilon'_{Au}(\lambda)$	Real part of the dielectric constant of gold, as $f(\lambda)$
$\epsilon'_m(\lambda)$	Real part of the effective dielectric constant of the matrix surrounding the gold nanoparticle, as $f(\lambda)$
θ	Angle between axis of radiation sensor and surface of glass
λ	Wavelength of light, nm
$\sigma_{thermal}$	Thermal stress
ϕ	Volume fraction of gold particles lying on the surface of the glass
ω_{l-}	Energy of symmetrically coupled plasmons on the inner and outer surfaces of the metal shell, eV
ω_s	Surface plasmon energy of a solid nanoparticle, eV
Subscripts	
a	Quantities associated with air
$b, back$	Back face of the glass
$conv$	Convective quantities

f	Front face of the glass
rad	Radiation quantities
$solar$	Solar quantities
Acronyms and abbreviations	
ASTM	American Society for Testing and Materials
ADF_t	Angular Distribution Function of transmittance
ADF_r	Angular Distribution Function of transmittance
CIE	International Commission on Illumination
E971	Standard Practice for Calculation of Photometric Transmittance and Reflectance of Materials to Solar Radiation.
FEA	Finite Element Analysis
G159	Standard Tables for References Solar Spectral
H_t	Haze parameters of transmission
H_r	Haze parameters of reflectance
ISO	International Organisation for Standardization
Kc	Fracture toughness
POB	Probability of Breakage
$Q_{convected}$	Energy convicted
R_{dif}	Diffusively reflectance of energy
R_{tot}	Total energy reflectance
SC	Shading Coefficient
SL	Solar Load
SHGC	Solar Heat Gain Coefficient
T_{dif}	Diffusively transmittance energy
T_{tot}	Total energy transmittance
TOMS	Tetraalkoxysilanes
TiO_2	Titanium dioxide
TSF	Thermal Stress Factor
U	Total heat transfer coefficient

Abstract

Reflective or absorptive coatings for solar control on windows are popular in the architectural and automotive industries. In general, noble metal coatings have been used in reflective applications, and various heat-absorbing dielectric compounds in absorptive ones. The ultimate objective is to moderate incoming infra-red radiation while simultaneously preserving the desirable transparent nature of the window. In addition, one problem with merely absorbing infra-red radiation by the glazing system is that the coating and hence the surface of the special glass becomes very hot. This increased glass temperature will result in thermal stresses leading to an expansion of the glass, which, if not matched by an expansion of the window frame, can cause buckling and cracking. The objective of this project has been to study heat transfer from and through glass surfaces to which IR-screening surface coatings have been applied, and to model the distribution of the resulting thermally-induced stresses in the glass.

The use of coatings of gold nano-particles in an absorptive role has hardly been considered previously. The present study explores the characteristics of such coatings by subjecting panes of various experimental and commercially available glasses to illumination by an array of incandescent lamps at 500 W/m^2, which is a representative figure for a vertical east- or west-facing window in Sydney, Australia or Houston, USA, during March and September. The heat transfer through the samples was determined and used to guide the subsequent finite element analysis. This provided an indication of the thermally induced stresses developed on the glass surfaces due to heat released by the absorptive coatings.

CHAPTER I - Introduction

It is believed that the first glass windows were made in Pompeii around 100 AD. For over a millennium glass had already been in production, but was not used for windows. Today basic soda-lime glass made of sand, limestone, and sodium carbonate is used in modern architectural buildings. Pilkington developed the twin ground polished plate system in 1938 while their float glass process was first launched on the UK market in 1959 [1].

Glass admits light and permits vision through it and at the same time it satisfies most of the requirements of an element in an exterior wall. In addition, it is durable in most environments, relatively low cost and is strong when properly used. Transparency of glass to visible radiation is the primary reason for its use in windows. However there may often be a requirement to control heat flow across a window.

Glass is not completely transparent to radiant energy, and some is reflected, some absorbed and the remainder is transmitted. The ratio of these factors is dependent upon the wavelength, incident angle of the radiation and the characteristics of the glass. Transmission through glass can be modified by changing the angle of incidence, by increasing the surface reflection by coating with reflecting coatings, or by increasing the absorption with absorptive coatings.

Until modern times little thought was given to the energy efficiency of window glass. However, as glazing areas continue to expand in modern buildings and in automotive design, control of heat transfer becomes a more significant factor. The continuing move towards better energy efficiency in buildings is providing a strong push for the application of coated glasses as they can be used in hot as well as cold climates. Solar radiation is short-wave (between 0.3 to 4.5 μm), and is made up of 43% visible light, 3% ultra-violet and 54% infra-red radiation of total energy, all of which produce heat when absorbed [2].

1

When the solar radiation enters the window the temperature inside the room rises and in summer the room may become unbearably hot unless cooled by an air conditioner. This is because un-coated glazing systems have poor thermal insulation properties. In combination with low emissivity coatings, multiple panel glazing systems are used in cold countries where conductive and radiative heat flow are reduced out of the window during winter, thereby reducing heating costs. However, this system is not suitable for tropical climates, as under such conditions much of the temperature rise (up to 90%) is due to infra-red radiation which may come from radiation transmitted through the window by direct solar illumination, while inwards conduction is less significant. An air conditioning system can remove this, but this may not be cost effective. However, blocking infra-red radiation with a solar control coating can potentially provide for more comfortable and energy efficient buildings in warm climates [3].

Windows with a high visible transmittance and a low shading coefficient are used in buildings which require significant cooling to achieve a pleasant environment, but are not energy efficient. For buildings with significant heating loads, coatings with low emissivity can be applied to minimize heat loss or gain through windows. It is desirable that glazing of this type lets in solar heat to offset winter heating system requirements, but prevents heat gain during summer.
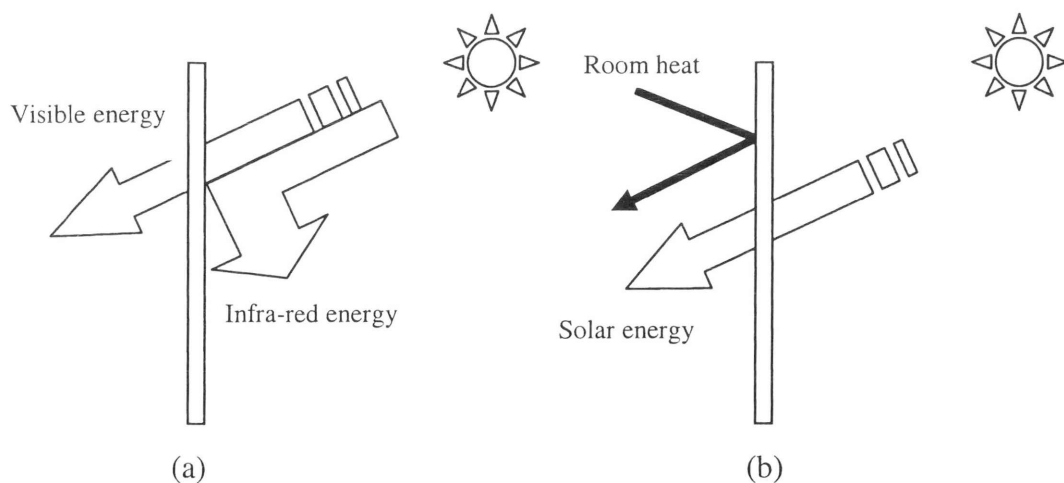
Figure 1. Characteristics of the ideal window in
(a) cooling and (b) heating dominated building

Several strategies can be adopted to minimize incoming solar radiation while simultaneously preserving the desirable transparent nature of the window. For example, a coating of material that reflects or absorbs a proportion of the solar radiation without absorbing or reflecting a significant portion of the visible light can be applied to the glass. This scheme of moderating incoming solar radiation is attractive when transmission of visible light must be effected as little as possible and attenuation is to be concentrated in the infra-red portion of the solar spectrum.

Solar energy transmittance (T_{sol}) is the integrated value of transmitted radiation while that of the reflectance (R_{sol}) is the integrated value of radiation reflected from the surface. Both are calculated from transmittance or reflectance spectra throughout the electro-magnetic spectra or measured using a radiation sensor and weighted by solar spectral distribution [3].

The proportion of the solar irradiance (T_{sol}) that is transmitted is [4]

$$T_{sol} = \frac{\int_0^\infty T_\lambda E_\lambda . d\lambda}{\int_0^\infty E_\lambda . d\lambda} \tag{1}$$

In which,

T_λ is the total spectral transmissivity of the glass, as $f(\lambda)$

E_λ is the spectral irradiance of the light source, $W.m^{-2}.nm^{-1}$, as $f(\lambda)$ and

λ is the wavelength of light, nm

Visible light transmittance (T_{vis}) as seen by the human eyes is the integrated value of the transmitted visible part of solar light which can be calculated as the proportion of the visible portion of the solar spectrum that is transmitted [4], that is,

$$T_{vis} = \frac{\int_{380}^{760} T_\lambda V_\lambda . E_\lambda . d\lambda}{\int_{380}^{760} V_\lambda . E_\lambda . d\lambda} \tag{2}$$

In which,

V_λ is the photo-optic luminous efficiency function of the human eye, as $f(\lambda)$

The limits of integration used in the above equations refer to the wavelength in nanometers.

The ratio T_{vis}/T_{sol} is a figure of merit used by many investigators [3] and provides the overall ability of the window to transmit visible light while blocking infra-red radiation and its maximum value is 2.08 for a perfect solar glaze using the photo-optic response given in ASTM E971 [5] and subjected to the Air Mass 1.5 spectrum specified in ASTM G159 [4]. This maximum value has been set by the natural properties of the sunlight received on Earth under various atmospheric conditions. For a dye-based coating values of 0.99 have been reported while for a metallised system a typical value is 1.04. For state-of-the-art spectrally selective films the ratio is between 1.7 to 1.9 [3, 6]. E_λ can also be taken as the output of an incandescent light by performing an analogous analysis with an artificial light, to provide a ratio $T_{vis}/T_{incan.}$

Energy absorbed by the material is in turn convected inwards and outwards with the relative proportions depending on the air temperatures and velocities of the corresponding external and internal environments. Some of the absorbed energy will also be subsequently radiated inward and outward.

Low-emissivity (low-e) glass reduces heat transfer back through the window with the help of special surface layer. Between 40% to 70% of the heat that is normally transmitted through the window is reflected by these coatings, while letting the full amount of visible light to pass through. Heat absorbing glass contains special tints that allow it to absorb as much as 45% of the incoming solar energy, reducing heat gain. Reflective glass is characterised by a reflective film and is applied to control solar heat gain during the summer [7].

Infrared reflective window coatings are widely used in cars and in buildings in order to increase the thermal comfort and to contribute to a more economic air conditioning system. In most cases infrared reflectance is achieved with nano-scaled metallic layers embedded in other dielectric thin films. The desired optical properties and mechanical and chemical stability depend on the design of the stack and the choice of materials. The choice of a certain technology is determined by a number of application specific issues both technical and economic. Highly reflective films are very good in heat rejection and

do not absorb much radiation. The use of these coatings in combination with double glazing systems can save about 30 to 40% of energy costs in residential and commercial buildings [8].

Unfortunately, reflective coatings are less popular for residential applications due to their relatively high costs and introduction of glare and unwelcome reflections onto neighbouring buildings. However, the difference between reflective and absorptive glass is that the window glass can become very hot in case of the latter type. A portion of absorbed heat will re-emit to both inside and outside of the glazing system due to a temperature difference between the glass and inside and outside environment with the amount determined by wind speed and air temperatures. Therefore the overall utility of these coatings depend critically on the ratio of these two effects. Absorptive systems are more cheaply made, by for example, simply incorporating an absorptive substance into the polymer layer of a laminate. Interestingly, in either case the actual cost of the raw material used is low, even if it is gold, at is no more than US\$3/m^2. Absorbing coatings are an attractive alternative to reflective coatings because the latter have a relatively high manufacturing cost (e.g. US\$10/m^2), due mainly to the need to amortize the cost of expensive vacuum equipment [9, 10].

In the present project, the heat transfer through various commercially available and experimental coated glasses were tested and compared under simulated hot climate conditions. The experimental coatings were based on gold nano-particles, and were prepared by Mr. Xu X, a PhD student from UTS. Since heat is absorbed by the glass it is not sufficient to determine that a glass perform adequately from the thermal and optical points of view. The absorbed energy will lead to an expansion of the glass, resulting in stresses that might cause the failure of the glass. It follows that there is a need to determine whether or not these glasses will fail. As a consequence an FEA analysis of the heated glasses was performed.

The structure of the thesis is as follows: The previous research work of other authors is reviewed in Chapter 2. The experimental set-up along with the measurement techniques, governing equations and theories involved are presented in Chapter 3. The results of the experiments are presented in Chapter 4. An overview of the issue of thermal stresses is given in Chapter 5. A discussion of thermal stress factor (TSF) and probability of breakage (POB) are presented in this chapter. Chapter 6 contains an analysis of stresses generated in the glass as a result of heating using finite element analysis (FEA). A case study for stress analysis using FEA method on a door-shaped glass panel is considered in this chapter. Finally, the results of this work are summarsied and are concluded in the Chapter 7.

CHAPTER II - Literature review

2.1. Background

2.1.1. Thermal Radiation Spectrum

Electromagnetic radiation, like all other forms of radiation, travels at the speed of light.
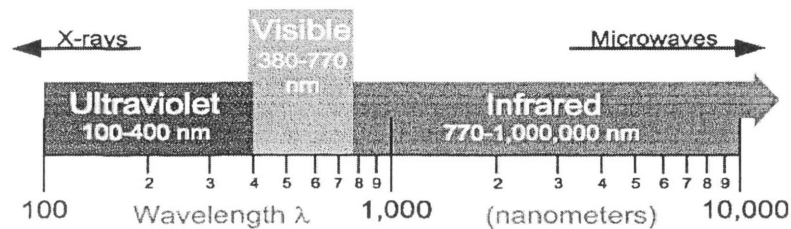
Figure 2. Thermal radiation portion of the electromagnetic spectrum [11]

There is no fundamental difference between light and other forms of radiation such as X-rays or radio waves. There is a difference only in the "eye of the beholder". A human eye can detect radiation if the wavelength is between 380nm and 750nm; radiation between these limits is called visible light. About half of the total energy of solar radiation is associated with the visible wavelength, the other half with wavelength longer than 750nm. This latter half is usually referred to as near infra-red radiation. The thermal spectrum spans a range of 0.1μm - 100μm, which, as shown in Fig. 2, includes the entire solar spectrum [11].

7

2.1.2 Optical properties of coated glass

A portion of the incident radiation from the light is transmitted through the glass while another portion is reflected. This transmitted or reflected radiation acts either specularly or diffusively. The wavelength dependent haze parameters for transmission and reflection are derived from the measurement of diffuse transmission and diffuse reflection respectively.

The haze parameter of transmission can be determined as the ratio of diffusive transmittance of the energy to the total energy transmittance [12].

$$H_t = T_{dif}/T_{tot} \qquad (3)$$

in which,

T_{dif} is the transmitted energy that is diffusively transmitted from the back surface

T_{tot} is the total energy that transmitted through

Similarly, a haze parameter of reflection can be defined as the ratio between diffusive reflectance of energy and total energy reflectance [12].

$$H_r = R_{dif}/R_{tot} \qquad (4)$$

in which,

R_{dif} is the transmitted energy that is diffusively reflected from the front surface

R_{tot} is the total energy that reflected from front surface
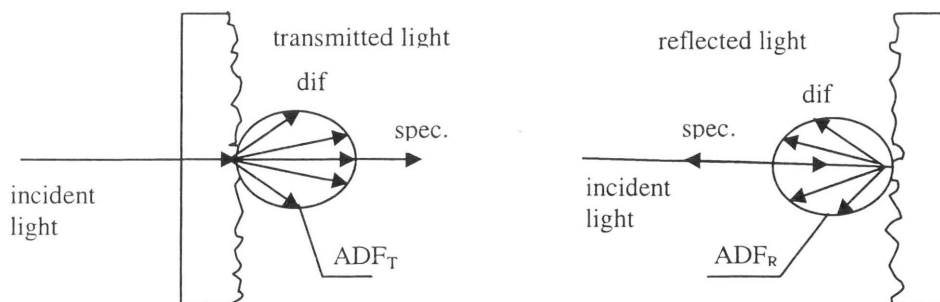
Figure 3. Scattering parameters for transmission
and reflection of the glass [12]

ADF$_T$ and ADF$_R$ (Fig. 3) are the angular distribution functions of transmittance and reflectance respectively [12].

2.1.3. Phong's Law

When a shiny surface of an object such as an apple is illuminated with a white light, a highlight on the surface is caused by specular reflection when light reflected from a surface has exactly same angle as its incident angle, whereas the light reflected from the rest of the apple is the result of diffuse reflection. Diffuse reflection is the change of the spatial distribution of a beam of radiation when it is reflected in many directions by surface. At the highlight the color appears to be the color of incident light, not the color of the surface of the object.
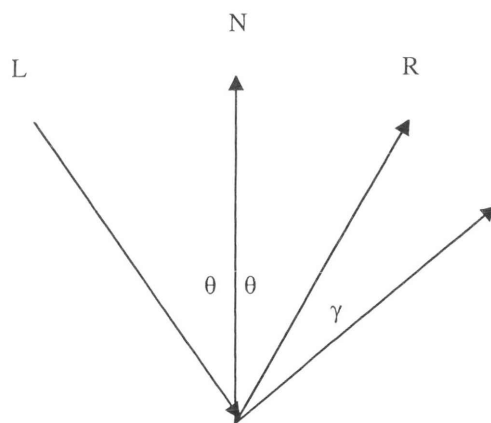
Figure 4. Specular reflection [13]

Here,

L is the incident light, R is the specularly reflected light, N is the normal and γ is the angular deviation from specular reflection.

A model called 'The Phong illumination model' [13] was developed by Phong Bui-Tuong for non-perfect reflectors. Phong assumed that maximum specular reflectance occurs when α is zero and falls off sharply as α increase (Fig. 4).

One way of describing reflection is to represent the intensity of the reflection beam as

$$I_\lambda \approx \cos^n \gamma \qquad (5)$$

In which γ is the angular deviation from specular reflection and n is the material constant. n has a large range, typically between 1 and several hundred [13]. As n increases the reflection decreases by eq. (5) is more and more specular.

2.2. Heat transfer

2.2.1. Heat transfer through glass window

Radiation: Heat is radiated from the sun through the air and is absorbed by the glass. The glass then re-radiates the heat inwards and outwards.

Inside   Outside

Conduction: Heat conducts from the warmer to the colder surfaces of the window.

Convection: The warm air first makes contact with the glass at the top of the window, and as it is cooled it moves downwards so that the air in contact with the glass becomes progressively colder as it approaches the bottom of

Figure 5. Three modes of heat transfer through a window in hot climates

Heat transfer through the window occurs by conduction and radiation. However, convection acts to increase the rate of heat transfer.

Conductive heat transfer takes place from more energetic particles of a substance to the adjacent less energetic ones as a result of vibrational interactions between the particles. In the case of a window it proceeds from the hot surface to the cooler one [14].

Heat transfer can be increased by convection, which is heat transfer via movement of the fluids surrounding the object. When only buoyancy forces set up by temperature differences cause the motion it is referred to as natural or free convection; but if it is caused by some other mechanism, such as a fan or pump, it is called forced convection.

Another mechanism for heat transfer is by radiation. Electromagnetic radiation emitted from a heat or light source as a consequence of its temperature is called thermal radiation. Ultraviolet, visible and infra-red radiations may all result from thermal radiation. The rate at which energy is emitted from a unit area of a surface is called the emissive power and it depends on the temperature and nature of the surface. A 'black body' has a surface which emits the maximum possible amount of radiation at any temperature. The emissivity of the real surface is the ratio of the emissive power of a real surface to the emissive power of a black surface at the same temperature. In contrast to heat transfer through convection and conduction, radiative heat transfer does not require a medium and can occur in a vacuum. The processes involved in the transfer of energy by radiation include emission, absorption, reflection and scattering [14]. An energy-efficient window designed for cold or hot climates minimizes heat loss or gain by controlling all sources of heat transfer.

Windows in cold climates transmit solar heat energy to the interior of the home. This energy from the sun enters in the form of short-wave infrared energy which is transmitted through the glass and is absorbed by the floors, walls, furniture, people, etc. This energy is then re-radiated by the floors, walls, furniture, etc. as long-wave infrared energy or heat [15].

The transmittance of solar heat through glass is measured by a quantity called Solar Heat Gain Coefficient (SHGC). It is defined as the fraction of solar heat that enters the window and becomes heat. This includes both directly transmitted and absorbed solar radiation. The lower the SHGC, the less solar heat that the window transmits through the glazing from the exterior to the interior, and the greater its shading ability. Heating by the sun in the Southern Hemisphere is concentrated along a home's east, north, or western-facing elevations [15].

The arrows in Fig.5 indicate the direction of the air movement over the window surfaces that occur during summer if natural convection prevails and the heat flows through the window from outside to inside. There is also a thermal radiation heat transfer between the window and environment [14].

Now that solar radiation and modes of heat transfer have been described it is now possible to discuss the properties of the window glasses and the existing methods of reducing heat transfer through a window.

2.3. Window glazing systems

2.3.1. Clear glass and its optical properties:

Ultraviolet Light Transmittance	80%
Visible Light Transmittance	90%

Clear glass transmits most of the infra-red portion of the solar radiation. Altogether, about 87% of the solar radiation is transmitted through the window glass. As a result the environment inside the room may become uncomfortable in a hot climate. On the other hand, heat from the room is transmitted through the clear glass to the outside in cold climates, and therefore the room become colder and uncomfortable. Therefore it is useful to control this heat transfer, without however destroying the transparency of the glass. Several strategies can be adopted. The various types of solar glazing that are prominent in the field of car and building industries will now be described.

2.3.2. Conventional solar glazing

Solar control window films are very thin polyester based products containing noble metals or dielectric compounds which are coated onto a glass to regulate transmittance of solar heat through the window. These films provide a good balance between heat loss and solar energy gain. This strategy of moderating incoming solar radiation is attractive

when transmission of visible light is to be affected as little as possible and attenuation is to be concentrated in the infra-red portion of the solar spectrum.

Applications of heat reflective and heat absorptive glazing in building and automobile industries are well known. Very good heat rejection is achieved by highly reflective systems, which do not absorb much radiation. For this reason windows that have been vacuum coated with nano-scale layers of gold or silver have been prominent in many city developments. Alternatively, other materials with appreciable densities of free electrons may be used as the reflector, for example TiN and ZrN, Cr_xN, Si_3N_4, SnO_2 or In_2O_3 [6].

On the other hand, absorptive glasses, by their nature, absorb the heat radiated from the sun and become hot. A portion of absorbed heat is then re-emitted to both inside and outside of the glazing system due to a temperature difference between the glass and inside and outside environment. The ratio of these two effects is therefore responsible for the overall utility of the coatings. Absorptive systems in current contention include FeO_x, indium tin oxide, antimony tin oxide, LaB_6, CoO_x, CrO_x, TiO_x, SeO_x, phthalocyanine dyes, and blends of rare earth hexaborides with indium and tin oxides [9, 10]. Typically, these would be used as, or in, coatings applied to the glass.

The advantages and disadvantages are discussed later in Section 2.5 of this Chapter but it is sufficient to say here that the greatest disadvantage is a loss of transparency in the glass.

2.3.3. "Clear" solar control glazing

Dai [3] investigated the spectral characteristics of solar control film that had been retrofitted onto windows in a tropical climate. Special selective films (Fig. 6) are highly efficient in rejecting solar radiation while keeping high visible light transmittance so as to introduce a "clear" solar control device. This is achieved by transmitting most of the solar radiation in the visible wavelength while reflecting the infra-red radiation. Electrically conductive layers such as thin silver films can be used as a selective coating. They found that the electron resonance in the conductive film leads to higher reflectivity in the infra-red range of the solar spectrum.
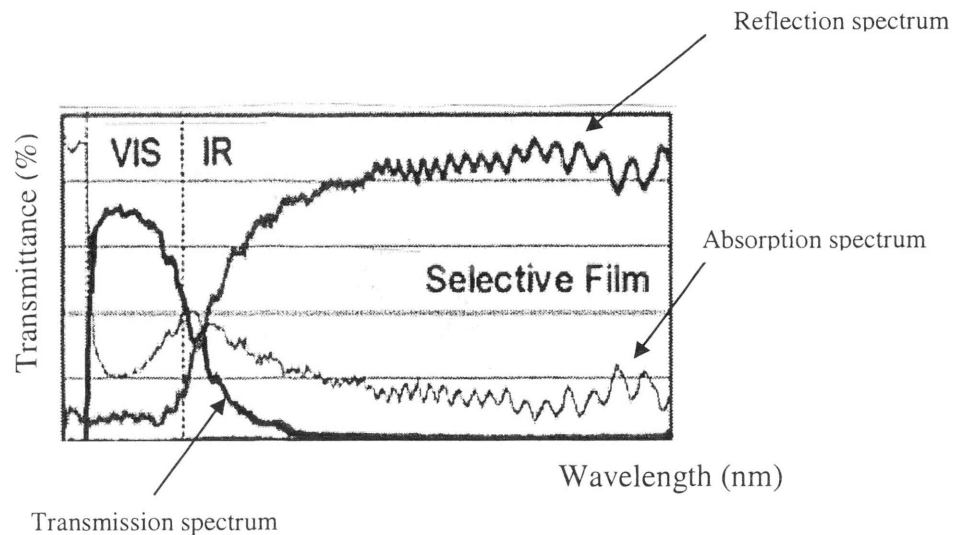
Figure 6. Spectral characteristics of selective film [3]

In Fig. 6 above VIS is represents the visible light region while IR represents the infra-red region. It can be seen from the figure that significant reduction of IR radiation by reflection contributes to low solar direct transmission, while low absorption is translated to low re-radiated heat. As a result, the special selective film provides the best solar heat control performance while staying highly transparent to visible light.

2.3.4. Other types of glazing

2.3.4.1. Antireflective glazing

Hofmann and Kursawe [16] discovered a new way to increase the energy efficiency of windows in cold climates by the usage of an antireflective coating. A suitable layer consists of nano-sized SiO_2 particles, with well defined diameters and porosity which is prepared by reactions of tetraalkoxysilanes (TOMS and TEOS) with ammonia and water in alcohol and alkoxyalcohol. This can significantly reduce reflectance of the incoming light and lead to higher transmittance and thus to higher energy efficiency (Fig.7) [16].

14
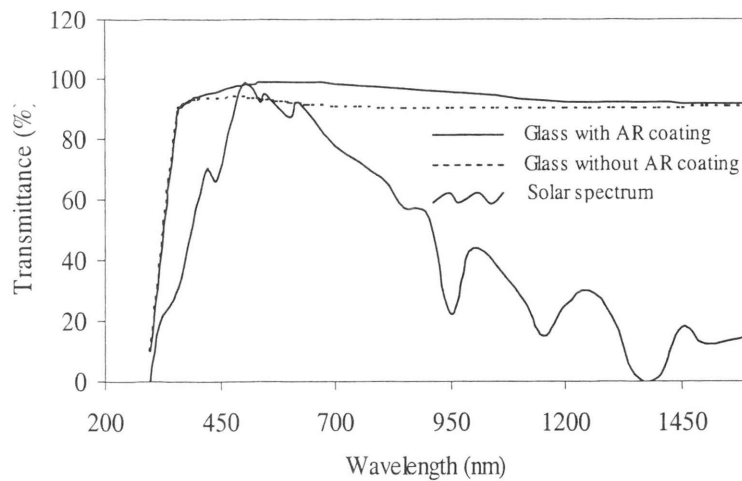
Figure 7. Transmittance behaviour of anti-reflective
coated vs. uncoated glass [16]

The wide band antireflective effect of the coating layer is demonstrated in Fig. 7. The
solar spectrum is almost completely covered by the transmission curve of the
antireflective coated glass. The solar transmittance can be enhanced by 6% in total over
the entire solar range [16].

2.3.4.2. Photocatalytic glazing

Optical properties such as scattering, reflection, absorption and transmission of
electromagnetic waves can be tailored by changing the structure of the glass. For
example, Huber and Proft [17] conducted experiments on the transmission of a titanium
dioxide (TiO_2) film. They found that titanium dioxide based photocatalytic transparent
"Active" glass with about 84% visibility transmittance coating (Fig. 8) exhibits self
cleaning and anti-fogging functions which could be very significant in future markets.
The catalytic action between incident sunlight and TiO_2 on the surface alters the surface
to super hydrophilic by creating oxygen vacancies on the surface. This is called the
"Lotus effect". Toughened glass, curved glass and otherwise coated glasses can be
coated using this technology [17].
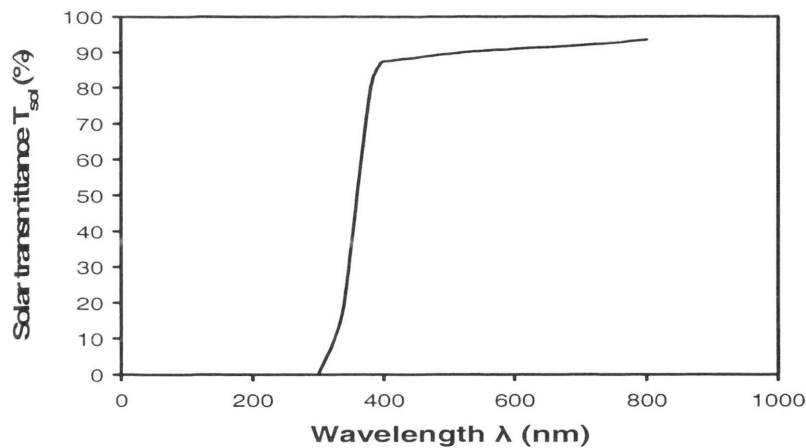
Figure 8. Transmission of TiO_2 film obtained from a TiO_2-Sol [17]

The visible transparency of the film shown in Fig.8 demonstrates a higher range transparency (400–800 nm) [17].

2.3.4.3. Variable transmission glazing

Wittkopf [19] has commented that the ideal optical and thermal properties of a glazing system change with changes in solar radiation condition during the day. A product to address this is called variable transmission glazing [18] or electro-chromic glazing (EC) [19]. Changes in properties can be achieved by applying electrical power to a glass pane. In one such system complementary electro-chromic layers consisting of Prussian Blue and tungsten oxide are coated to two glass panes with a transparent electro-conductive film (e.g. fluorine-doped tin oxide). The two panes are laminated together with an ion conductive polymer foil. If 1.2 V to 2.4 V d.c. voltage is applied, oxidation and reduction reactions in the electro-chromic layers are induced which are accompanied by insertion or extraction of ions. This process leads to a change in the transmittance of visible light and near infra-red radiation for these layers [19].

16
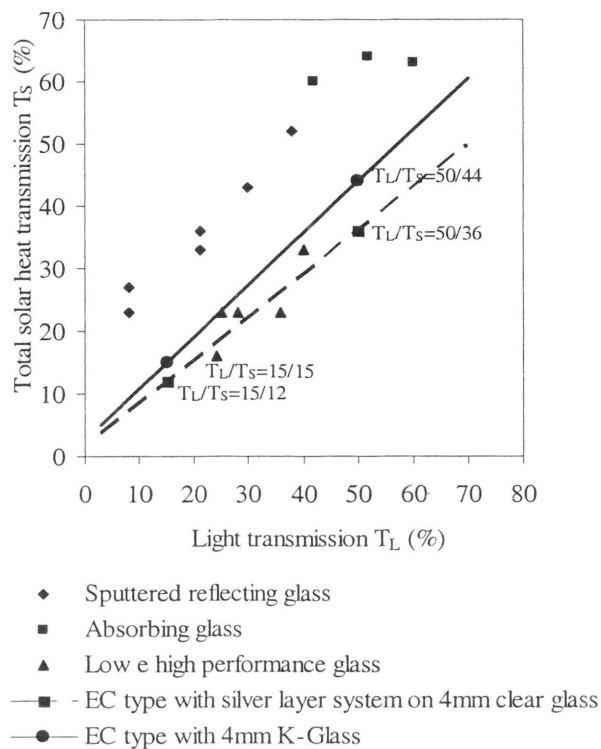
Figure 9. Visible light transmission through variable transmission window system vs. various other glazing systems as a function of total energy transmission [18].

The T_S vs. T_L diagram for both types of electro-chromic glasses (EC) in relation to conventional low emissivity or solar control glazing are shown in the Fig. 9. The glazing with variable transmission is represented by two lines between the T_L/T_S values in bleached or dark state while a conventional glazing is a single dot within the diagram. The light transmittance can be varied between 50 and 15% in 4 to 6 minutes giving a modulation factor of 3.3. It is cleared from Fig. 9 that the heat transmittance characteristics of the conventional absorptive glazing have been changed by using electro-chromic glazing technology. It can also be seen from Fig. 9 that electro-chromic glass with silver layer on 4 mm glass has a higher energy transmittance ability than the simpler kind.

Variable light transmission glazing can be used to optimize day lighting as well as to optimize energy needed to control a desire temperature and lighting level.

2.3.5. Solar glazing based on gold nano-particles.

Gold nanoparticles can absorb light by the well-known process of plasmon resonance, and this idea has been tested out for solar glazing by by fellow student Mr X. Xu [20]. However, the plasmon resonance of his coatings does not appear to be in the optimal position, even though it has been considerably red-shifted from the 518 nm of isolated gold nano-particles. A peak would be more desirable that would have been red-shifted even further towards or into the near-infrared. In theory by increasing the surface coverage (ϕ), some progress in this direction may be made since the condition for plasmonic resonance is given by [20]

$$\varepsilon'_{Au}(\lambda) = -\varepsilon'_m(\lambda)\frac{(2+\phi)}{(1-\phi)} \tag{6}$$

Where, ϕ is the volume fraction of the gold particles.

However, in reality, due to the rapid decrease in the transparency of such dense coatings, an increase in volume fraction cannot be used to shift the wavelength of maximum absorption to more than about 700 nm [21, 22].

The use of hemispheres in coatings is only one of the possibilities. The plasmon resonance of gold nano-particles is particularly sensitive to shape [23]. Gold nanoshells, for example, have interesting optical properties. Here the wavelength of maximum absorption of the coating is a function of the ratio (x) of the inner and outer radii of the gold shell [24]:

$$\omega_{l-}^2 = \omega_s^2\left[1 - \frac{1}{2l+1}\sqrt{1 + 4l(l+1)x^{2l+1}}\right] \tag{7}$$

It must be noted here that the derivation holds true for particles much smaller than the wavelength of light. When diameter of particles exceed, say 200 nm, the light will be scattered and thus a coating could display a hazy appearance in the visible spectrum. Unfortunately, a suitably cheap method of producing these tiny structures in broader

scale has not been achieved. However, small quantities have been made under laboratory conditions.

2.4. Properties of window glazing

2.4.1. Solar thermal properties

The heat flow is given by:

$$Q_a = Fl_t + U(t_0 - t_i) \tag{8}$$

where l_t is the solar radiation incident on a vertical surface of a specific location, F is the Solar Heat Gain Coefficient which is the proportion of directly transmitted and absorbed solar energy that enters into the building interior, U, the total Heat Transfer Coefficient is the value of the measure of air to air heat transfer due to thermal conductance and the difference between indoor and outdoor temperature $(t_0 - t_i)$.
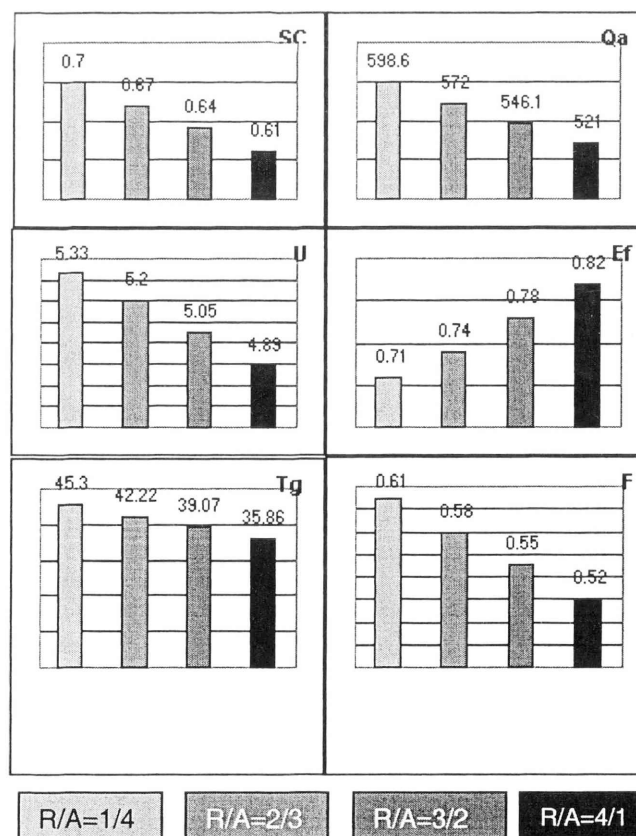
Figure 10. Various modes of solar thermal properties using a model film at same solar direct transmittance but different reflectance/absorption ratio (R/A) [3]

19

Dai [3] has investigated the optical properties of the film in terms of Solar Heat Gain Coefficient, Shading Coefficient, U factor and other optical/thermal properties as combinations of film and substrate glass. He found that the films make a very large difference in solar energy admittance when applied to glazing systems. The effect is shown in terms of glazing system, solar heat gain coefficient, Shading coefficient, total heat transfer coefficient and other optical/thermal properties. Solar energy rejection can be achieved by both absorption and reflection.

The properties evaluated in the Fig.10 are based on the ratio of the reflection to the absorption (R/A). Different ratio gives different values in terms of Shading coefficient, Total heat transfer coefficient, Total heat admission, and glass Temperature. For example; when reflection vs. absorption ratio is 4:1 the glass temperature is 35.86°C, when it is 3:2 the temperature value is 39.06°C, while at 2:3 ratio temperature is 42.22°C and finally when ratio is 1:4 the temperature value is 45.3°C. The differences made by solar rejection mode in the Fig.10 shows that when reflection portion is increased at the same value of solar transmittance, Total Heat Transfer Coefficient U, total heat admission (Q_a), Shading Coefficient (SC) and glass temperature (T_g) are reduced, resulting in higher efficiency [3].

2.5. Advantages and disadvantages associated with window glazing systems

2.5.1. Advantages

- Tinted, reflective and spectrally selective glazings can all reduce solar heat gain;

- Spectrally selective glazings let in the most visible light;

- A gas-filled multi-layered low-e window with a good frame is good in cold climates;

- Tints and reflective glazings can give a building a pleasant appearance.

2.5.2. Disadvantages

Heat rejection:

• Reflective coatings induce glare and unwelcome reflections onto neighbouring buildings;

• The metallic lustre and relatively high costs (>U$10/m^2) of reflective coatings may make them unsuitable for residential applications

• Low light transmittance leads to increased lighting requirements.

Heat absorption:

• Less efficient since a proportion of the energy that they absorb is convected from the back face into the interior of the building;

• Absorbing tints have a colour and for consistence must be applied to all faces of the building which is not economic.

2.6. Opportunities in window glazing

The literature review has indicated that many authors have contributed in the analysis of the performance of solar glazing systems. The physics of the problems is generally understood but the thermal phenomena that occur in the coated window glass seem to have been neglected. The major concern of the present study is to investigate these effects and role of the other parameters that influence heat transfer, and to relate this to the question of stress development in the glass.

In the next chapter I will describe the experimental rig and measurement processes used for the investigation.

CHAPTER III - Experimental set-up

3.1. Physical model

A schematic illustration of a 3 mm glass sheet with a solar control coating is shown in Fig.11. The incident heat radiation flux is normal to the glazing with a constant value of, for example, 500 W/m². The initial interior and exterior temperatures are initially set constant, but start changing soon after the light source is switched on. The thermo-physical properties of the glass are considered constant. The values of convective heat transfer co-efficient for exterior and interior sides must be determined, following which the net energy flows through the coated glass panes are calculated. The effects of absorption in the film coatings are considered.
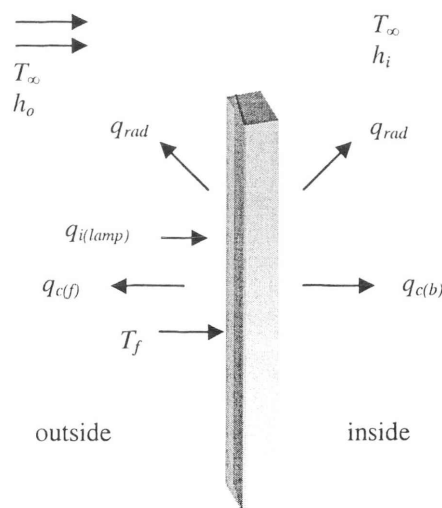
Figure 11. Physical model of glass with solar control coating system

3.2. Heat balance across the window

The heat balance takes into account the three fundamental modes of heat transfer: conduction through the glass, convection to air, and short and long wave radiation from solar radiation entering through the window and interchanges with radiation sources such as surrounding surfaces, equipment and people.

The energy balance in 3mm single glazing is shown in Fig.12 below.

Front face temperature $T_{S(f)}$ Back face temperature $T_{S(b)}$

Radiation incident (q_i)

Direct solar transmittance q_t

Radiation reflected (q_r)

Total heat transmitted

Total heat rejected

Heat convected outwards (q_{co}) Heat convected inwards (q_{ci})
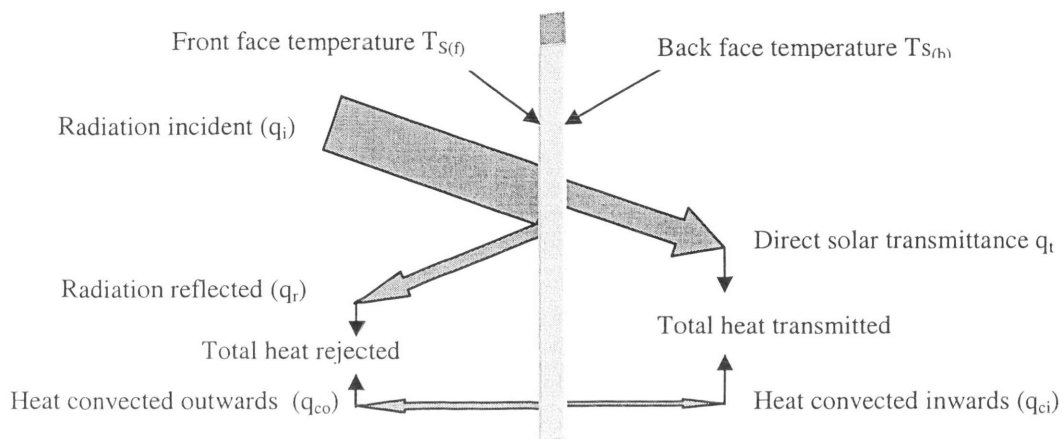
Figure 12. Energy balance in the glass

Energy balancing equation:

$$q_{incident} = q_{reflected} + q_{transmitted} + q_{convected(f)} + q_{convected(b)} + q_{radiated(f)} + q_{radiated(b)} \qquad (9)$$

Where *(f)* and *(b)* refer to the front and back faces of the glass respectively.
Energy incident on the surface and energy reflected from the surface and energy transmitted through the surface are measured with a radiation sensor.

Energy convected $(Q_{convected})$ can be determined from Newton's Law of Cooling which is [26],

$$Q_{convected} = (T_s - T_{air}) * A * h \qquad (10)$$

In which h is the heat transfer coefficient in Watts/m^2/^{0}C and A is the area of the glass.

The heat transfer co-efficient h has been determined by others from experiment, and correlations are then constructed which may be more or less accurate [26]

$$h = (Nu_L \times k)/L \ (Watts/m^2/^0C) \qquad (11)$$

An example is given in Appendix E.

For cooling by free convection along a vertical flat plate, the Nusselt number Nu_L can be obtained from the Prandtl (Pr), Raleigh (Ra) and Grashof (Gr_L) numbers from the correlation [26]:

Nusselt number is the dimensionless heat transfer coefficient and is defined as hL/k where, h is the heat transfer coefficient, L is a characteristic length and k is the thermal conductivity.

$$\text{Nusselt number } Nu_L = \left\{ 0.825 + \frac{0.387 Ra^{1/6}}{\left[1 + (0.492/\Pr)^{9/16}\right]^{8/27}} \right\}^2 , for\ 0.1 < Ra < 10^{12} \ [35] \qquad (12)$$

A correlation that may be applied over the entire range of R_a which gives a mean Nusselt number over the vertical plate [27]

Raleigh number Ra is the non-dimensional ratio between the product of buoyancy forces and heat advection and the product of viscous forces and heat conduction in a fluid :

$$Ra = Gr_L.Pr \qquad (13)$$

in which, Grashof number Gr_L is the ratio of buoyancy forces to the viscous forces. Prandtl number Pr is the ratio of momentum diffusivity (kinematic viscosity) to thermal diffusivity.

3.3. Apparatus for determining energy balance

$0.25 \times 0.25 m^2$ glass panes were placed in an open wooden frame facing an array of incandescent lights. The air flowed though the front to the back so that air temperature inside and outside remained same as laboratory temperature. The distance between the light and the glass pane was adjusted so that a uniform irradiance of 500 W/m^2 fell on the position to be occupied by the glass pane. 500 W/m^2 is a representative figure for a vertical east- or west-facing window in Sydney or Houston during March and September [28]. A schematic diagram of the experimental set-up is shown in Fig.13. The colour temperature of such lights is 2800K in comparison to that of sun which varies between about 5500K and 6500K at noon depending on atmospheric conditions. Therefore, such lamps do not simulate the solar spectrum exactly.

(a)
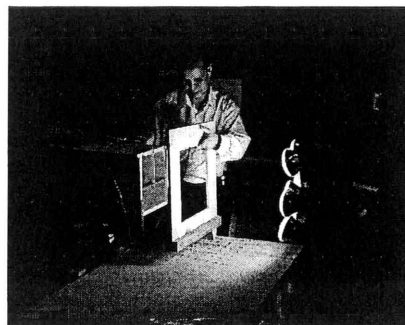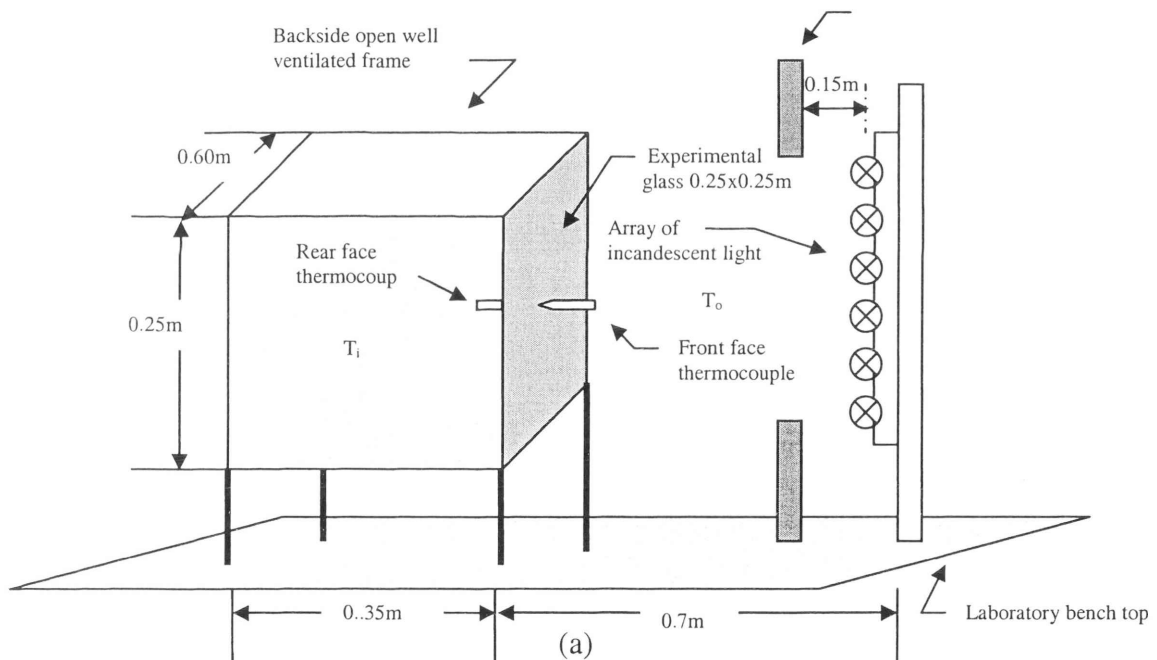
(b)

Figure 13. (a) Schematic representation of experimental set-up, (b) Photograph - Measurement of radiant heat transfer through coated glass panes.

25

The spectrum of these lamps is richer in infrared (e.g. Illuminant A of standard ISO 10526:1999 [29]) than that of the sun as shown in Fig. 14. However, comparative assessment and ranking of the various glazing systems using such an array of lights is useful because of the difficulties in dealing with the variability of real solar illumination. To eliminate excess illumination from the experimental apparatus a wooden screen with a square cutout of 0.3 m side was placed between the glass and the light source, 30 cm away from the light. The heat flux from the lamps was measured with a thermopile detector (PMA 1143) from Solar Light Co USA (Appendix A). The detector provides a linear response to the sum of all radiation received between wavelengths of 200 and 50,000 nm with a measurement zone of an angular width of 10°. The sensor produced a voltage output, which was proportional to the intensity of radiation incident upon the sensor. A voltmeter was connected to the sensor to monitor the output. The temperatures of the inner and outer surfaces of the glass sheet were monitored using thermocouples as well as a Mini Surface Thermometer from Testo Australia. The thermocouples were placed in the middle of the front and back face of the glass.
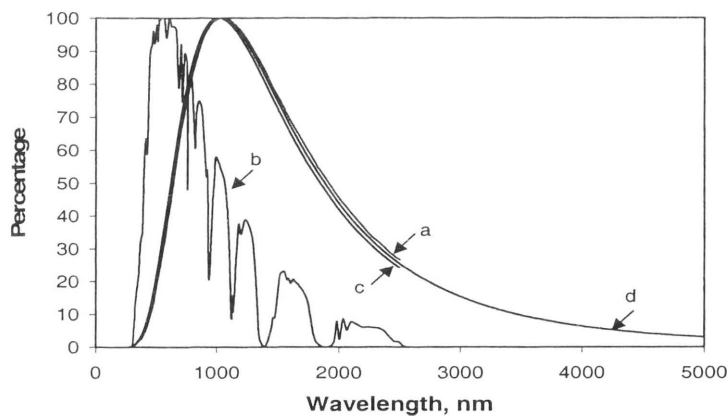
Figure 14. Spectral characteristics compared of (a) incandescent lamps used, (b) ASTM's AM 1.5 solar spectrum, (c) CIE/ISO Illuminant A and, (d) black body at 2800K. (Data for lamps from Philips Corporation).

3.4. Materials included in the test matrix

3.4.1. Standard materials

Verification of the radiative and optical performance of the apparatus, as well as the novel coatings, was done by testing and ranking certain standard materials, for which the relevant solar performances are known. These were

1). A pane of standard 3 mm thick clear window glass

2). A 6 mm thick pane of laminated solar tinted glass ('XL121' from manufacturer G James Body Tint Australia Pty Ltd)

3). Two sheets of 3 mm glass coated with self-adhesive solar films ('$V_K 40$' and '$V_K 70$') from V-Kool Inc of Houston, Texas

4). 'PNTHR 50 Scotchtint' (from 3M) tinted on 3mm pane

5). A sheet of 6.38 mm 'ACTIV' glass from Pilkington (Australia) Limited.

Selection of these five materials provided a reasonable sampling of currently available products.

3.4.2. Coating of glass panes at UTS

Two glass panes were coated with gold nano-particles using a modified electrolysis deposition solution based on $HAuCl_4$ and ethylene diamine with hydrazine as a reductant according to a process devised and carried out by fellow student Mr X. Xu [22]. A series of test coupons were coated and immersed in the bath each separately for a successively longer time to determine the range of coating colours for the present experiment. The test coupons were standard glass microscope slides of 1.0 mm thickness. It was necessary to scale-up the technique significantly for the application to sheets of glass measuring 0.25 by 0.25m. The panes were first pre-treated by immersion in 2 litres of buffered hydrofluoric acid containing 40g NH_4HF_2, 10ml (49%) HF and

200ml concentrated hydrochloric acid (37%) for 1 minute. The glass was then rinsed and immersed in 0.1% $SnCl_2$ in water for 2 minutes. Thus nanoscale sites were created upon which the gold could be nucleated later. Before deposition of the gold the glass was rinsed again with pure water. The gold was then deposited from 3 L solution of 0.0004 M $HAuCl_4$, 0.015 M N_2H_4 and 0.03 M ethylene diamine This solution was made up with pH 8.0 buffer solution, which was prepared by mixing 2000 ml 0.025 M $Na_2B_4O_7.10H_2O$ (borax) with 820 ml 0.1 M HCl. The two glass panes designated 'Au-1' and 'Au-2', were kept in this solution for 10 and 20 minutes respectively. The pH of solution was constant during the deposition.
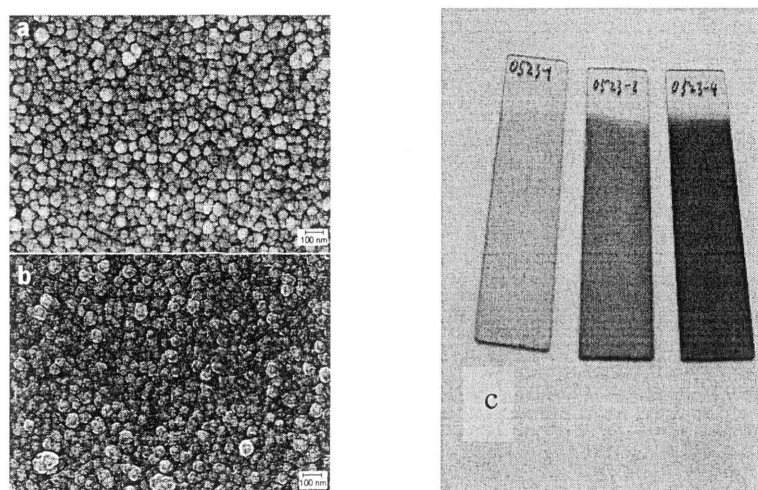
Figure 15. a) and b) High resolution scanning electron microscopy images of coatings on sample *Au-1* and sample *Au-2* respectively showing a distribution of nano-sized gold hemispheres of ~30 nm diameter and c) slides with range of coating colors (photos courtesy of Mr X. Xu).

3.5. Measurements

The whole glass pane was split into a number of concentric regions (rings shown in Fig.16) and ranking of the glasses was achieved by measuring the average value of heat transfer through various locations of each individual ring as shown in Fig. 16, and then summing the data for all the rings (Fig. 16). This provided an aggregated result for the whole pane. Measurements at the four corners of the glass (Fig.16) indicated that the flux was approximately equal over the extent of each annulus.

Energy falling per sq meter on each region W/m^2
Region 1 = 500
Region 2 = 500
Region 3 = 479
Region 4 = 471
Region 5 = 432
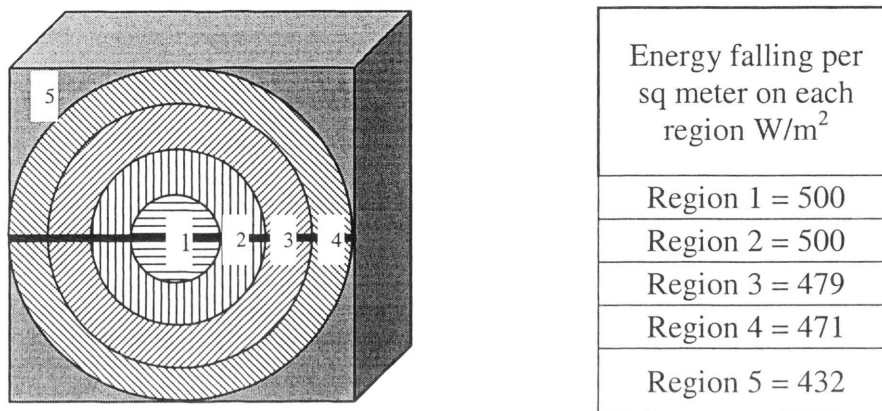
Figure 16. Measurement of incident radiation
from the regions mapped onto the pane

With the glass pane removed total radiation that was incident at 90° was measured first by placing the sensor at the appropriate position within the rig and pointing it towards the light source in each case (Fig. 16). A total of 29W of energy was received by the panes (Appendix B). The glass panes were put back in place and radiation transmitted at 90° through the glass was measured in similar way (Appendix C).

In the centre the irradiance was 500 W/m^2 but it declined as towards the edges of the glass (see Fig.16). The measurement error was found to be of the order of 4% by means of an energy balance (see Table 1, Chapter 4).
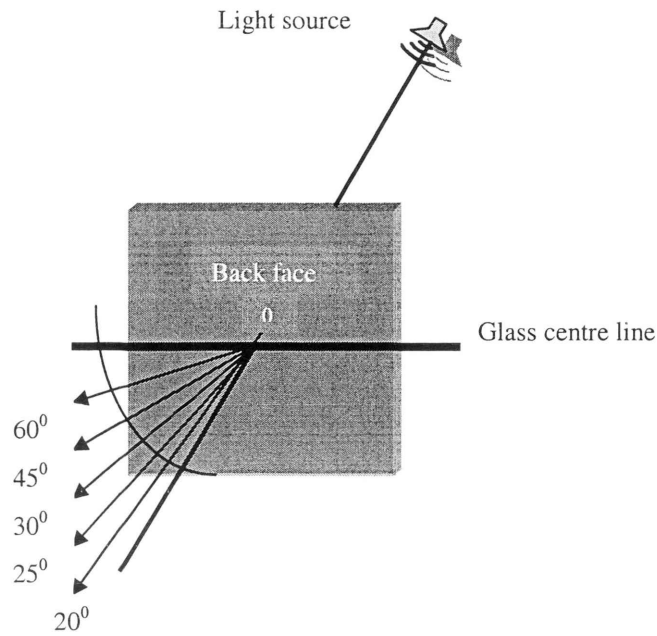
Figure 17. Measurement of radiation that was specularly and diffusively emitted from back face

A series of measurements were taken at a varying values of θ for each region of the surface to determine radiation that was diffusively emitted out of the front and back faces at an angle of incidence of greater than $0°$ (Fig. 17 from the back face and Fig. 18 from the front face). However, placement of the sensor on the $0°$ direction for the front face was not possible due to the shadow that it cast onto the glass. In that case, measurements were taken by progressively moving the sensor along a level of increasing distances from the glass, and at angles of incidence chosen so that the measured region was not shadowed.
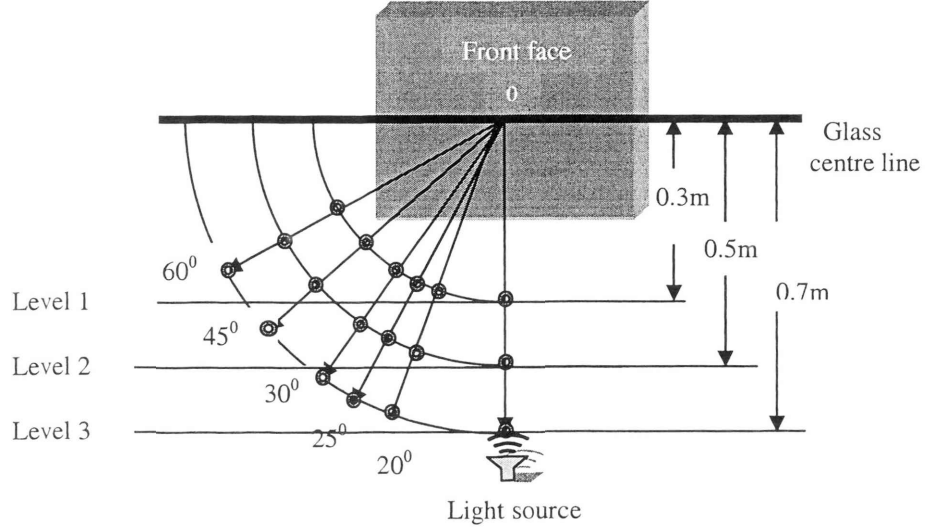
Figure 18. Measurement of radiation that were
specularly and diffusively emitted from front face

It was found that the intensity of radiation at a fixed distance r from the glass surface fell with increasing angle θ approximately according to Phong's Illumination Model [13] (Appendix D).

$$D_\theta = D_{r,0} \, [cos(\theta)]^n \tag{14}$$

Whereas at a fixed angle the intensity fell off with distance in an approximately linear fashion

$$D_r = D_{0,\theta} - a.r \tag{15}$$

(The well-known r^{-2} dependency does not apply here because the glass sheet is not a point source). An empirical model for radiation leaving the glass surface as a function of distance and angle is produced by combining these two phenomena, viz,

$$D_{r,\theta} = (D_{0,0} - ar)[cos \, (\theta)]^n \tag{16}$$

Values of a and n for equation (16) were found and the value of $l_{0,0}$ could be found from this by extrapolation, Fig.19. Similar measurements and calculations were repeated for

31

all types of glass sheets. However, a poor fit was obtained for the highly reflective sample V_K 40.
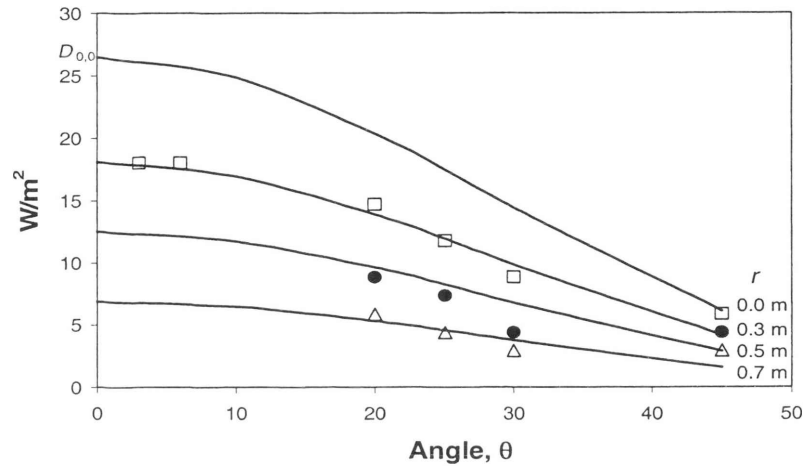
Figure 19. Empirical model for diffusively emitted radiation from the front surface of a plain glass sheet, showing how the emission, $D_{0,0}$, normal to the plane of glass was estimated by extrapolation.

A similar procedure was used to re-record the diffusive radiation for the back face of the glass. The sum of radiation reflected by the glass and the thermal radiation that was diffusively emitted from the front face are listed in Table 1, Chapter 4. Similarly, diffusively emitted radiation in the case of back face is the sum of both the thermal radiation off the heated surface, and any other transmitted radiation that has been transmitted at other than the $90°$ direction by the glass.

The heat transfer co-efficient h was estimated from Eq. (11) and for cooling by free convection along a vertical flat plate, Nusselt number Nu_L was obtained from the Prandtl, Raleigh and Grashof numbers from the relationships Eqs. (12) and (13).

With the conditions applicable here, Pr for air is fairly constant at 0.71, and Ra is about 3×10^7.

Calculation for h was carried out for all the glass samples individually (Appendix E) using measured surface temperatures. This has yielded values of h close to 5 $Wm^{-2}K^{-1}$ for all glass samples (Appendix F), in agreement with estimates from consideration of an energy balance Eq. (9).

The heat convected from the front and back surfaces of the glass was estimated from Eq. (10) (Appendix G).

If the temperature measured was in error by $-1^{o}C$ then h would have decreased by 1.6%, conversely, if the temperature measured was in error by $+1^{o}C$ then h would have increased by 1.4%.

The work described in this chapter provided the means to test and rank the various types of solar glazing. The results will be discussed in the next chapter.

CHAPTER IV - Results

4.1. Heat transfer across glass

Under steady state conditions, all heat absorbed in the glass must be transferred outwards and inwards by a combination of convection and radiation. It can be seen from Table 1 that XL121 Optilight 6mm laminated product and PNTHR50 Scotchtint film on 3mm glass are comparatively strong heat absorbers whereas V_k-multi-layered sputter coated film on 3mm glass is simultaneously both strongly reflective and absorptive. Pilkington Aktiv film on 3 mm glass is also a moderate heat absorber with a strong capacity of transmittance in the visible wavelengths.

Table 1. Energy balance for a 29 watt heat load with tungsten 2800K radiation applied to a variety of glazing systems at intensity of 500 W/m^2. The error on values of $D_{0,0}$ is <0.1 W with the only exception being the sample V_K 40. The energy balance is accurate to within 1.2 W (4%).

Glass type	Temperature °C		Radiation transmitted		Radiation reflected, $D_{0,0}$		Convected energy, front face		Convected energy, back face		Not accounted for	
	Front	Back	W	%	W	%	W	%	W	%	W	%
Clear	32	31	24.2	83	1.6	6	2.5	9	1.9	5	-1.2	-4.1
XL121	45	42	14.7	51	1.7	6	7.5	26	6.3	22	-1.2	-4.1
PNTHR	43	41	14.1	49	2.6	9	6.4	22	5.8	20	0.1	0.4
V_K40	39	37	2.3	8	17.5	60	4.8	17	4.1	14	0.3	1.0
Aktiv	40	39	17.2	59	1.7	6	5.4	19	5.1	18	-0.4	-1.4
Au-1	37	36	20.0	67	2.0	7	3.8	13	3.5	12	-0.3	-1.0
Au-2	41	38	17.2	59	2.0	7	5.8	20	4.5	16	-0.5	-1.7

Samples *Au-1* and *Au-2,* coated with gold nano particles at UTS were absorptive in nature converting 25% and 36% respectively of the incoming radiation to heat.

34
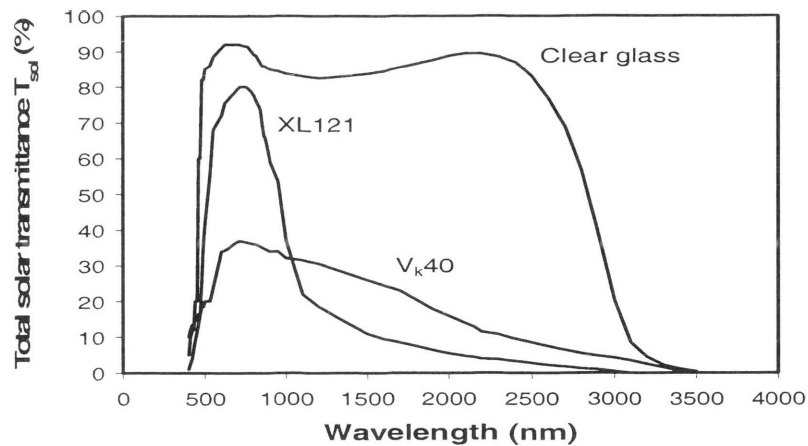
Figure 20. Transmission as a function of wavelength for commercial glasses XL121 and V_k40. Data are from the manufacturers' pamphlets.

Spectral behaviour of two of the commercial coated glasses is outlined in Fig. 20. It can be seen that XL121 has a high level of visible light transmittance but provides good protection against the transmission of uncomfortable infrared radiation. On the other hand contribution in transmittance of visible light by V_{kool} type appears to be comparatively lower but it rejects a high percentage of infrared radiation by reflection and keeps the room cool in a hot climate.
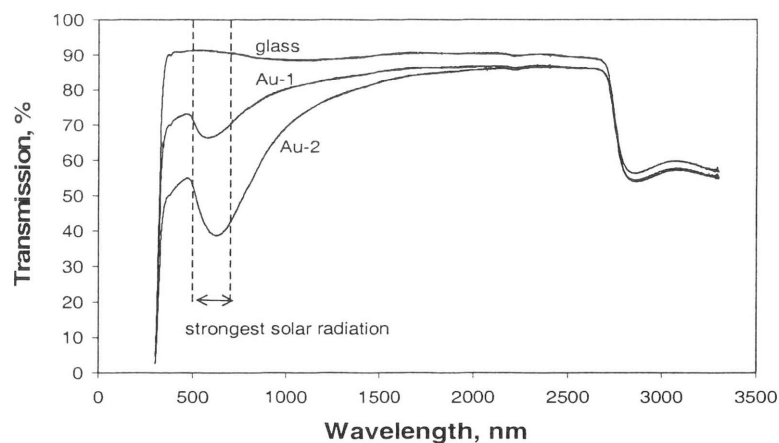
Figure 21. Transmission characteristics of two gold coated panes (*Au-1* and *Au-2*). The spectrum of ordinary window glass is also shown. Data are from X. Xu and reference [22].

35

The visible-infrared transmission spectra of test coupons corresponding most closely with glass panes *Au-1* and *Au-2* are shown in Fig. 21. It may be seen that the minimum wavelength of the transmitted radiation for coating *Au-1* is at about 615 nm. If Fig. 13 is compared with Fig. 21 it can be seen that wavelength of strongest absorption is within the region of strongest intensity of solar radiation, which can be considered to lie roughly between about 500 and 700 nm. The peak in absorption spectrum of coating *Au-2* lies at about 660 nm and is shifted further into the near infra-red. Accounting for the 3mm glass thickness illuminated with Illuminant A and applying the analogous version of Eqs. (1) and (2), T_{vis}, T_{lamp} parameters predicted for panes *Au-1* and *Au-2*, are found to be 0.63 and 0.74, and 0.41 and 0.68, respectively. Since the wavelength of strongest output of the lamp illumination is shifted away from the spectral position of maximum absorption of the gold nano particles, the results are not as favorable as for sunlight.

It was shown that 'radiation transmitted' is the sum of $q_{transmitted}$ and $q_{radiated(b)}$. Similarly, 'radiation reflected' is the total of $q_{reflected}$ and $q_{radiated(f)}$. Therefore, the contribution of energy radiated from the glass as well as the aggregated contribution of diverse measurement errors must be reflected in the column 'Not accounted for' in the Table 1. It is clear that since this is a steady state test the residual, unaccounted for, diffuse component of the radiation is less than 1.2% in these tests.

4.2. Solar Heat Gain Coefficient *(SHGC)*

The parameter F known as the 'Heat Gain Coefficient' [3] is the proportion of the incident energy that is ultimately transferred to the internal environment which is

$$F = \frac{q_{transmitted} + q_{convected(b)} + q_{radiated(b)}}{q_{incident}} \qquad (17)$$

If $q_{incident}$ is solar radiation then $F=F_{solar}$,

36

The value of F was increased greatly because of the still air conditions of the test used in the laboratory. Nearly half of the absorbed energy was re-transmitted into the simulated interior environment by convection from the back face of the glass (see for example Table 1).

The values of F_{solar} provided by the suppliers are compared with measured values of F_{lamp} listed in Table 2 for the same materials. A strong correlation between the values of F_{lamp} measured in the present work and the published F_{solar} figures for the various reference samples has been observed and is expressed here as a polynomial.

$$F_{solar} \approx \sum_{i=0}^{2} (a_i)^i F_{lamp} \qquad (18)$$

where $a_0=0.287$, $a_1=0.1734$, $a_2=0.5337$, $R^2=0.9943$, and $0.3<F_{lamp}<0.9$

This relationship has been used in Table 2 to provide estimates of F_{solar} for the tested glazing materials. Thus various glazing systems can be roughly compared under approximately solar conditions. The ratios of total energy transmitted by each sample to that transmitted by clear 3 mm glass shown in the Table 2 is equal to the so-called 'Shading Coefficient' in the case of solar illumination.

It is clear from the analysis of the data in Tables 1 and Table 2 that all of the solar glazing coatings tested were highly absorptive in nature, blocking between 25% (Au-1) and 48% (XL121) of the incoming radiation.

The radiation not transmitted was either absorbed and converted to heat, or reflected, as shown in the Table 1 of this Chapter.

Table 2. Performance data provided by the material suppliers for performance in sunlight compared to the proportion of total energy transmitted by the test samples (Solar Heat Gain Coefficient) using the Illuminant A spectrum. Transmittance data have an accuracy of ±1%.

Material	Source	Total energy transmitted, F	Ratio relative to clear 3 mm glass
3 mm glass	F_{lamp} (measured)	88%	1.0
	F_{solar} (estimated)	85%	1.0
	F_{solar} (supplier's data)	86%	1.0
XL121	F_{lamp} (measured)	73%	0.83
	F_{solar} (estimated)	70%	0.82
	F_{solar} (supplier's data)	69%	0.80
PNTHR50	F_{lamp} (measured)	69%	0.78
	F_{solar} (estimated)	66%	0.78
	F_{solar} (supplier's data)	68%	0.79
VKOOL 40	F_{lamp} (measured)	22%	0.25
	F_{solar} (estimated)	35%	0.41
	F_{solar} (supplier's data)	35%	0.42
Activ glass	F_{lamp} (measured)	77%	0.88
	F_{solar} (estimated)	74%	0.87
	F_{solar} (supplier's data)	72%	0.88
Au-1	F_{lamp} (measured)	79%	0.97
	F_{solar} (estimated)	76%	0.89
Au-2	F_{lamp} (measured)	75%	0.84
	F_{solar} (estimated)	72%	0.85

4.3. Energy balance for experimental glazing

The outcomes of the experiments listed above were used to balance total energy distribution on each type of glass from Eq. (9).

6mm

Incident light
100%

Reflected
6%

Transmitted
51%

Convected
outward 26%

Convected
inward 22%

a)

3mm

Incident light
100%

Reflected
60%

Transmitted
8%

Convected
outward 17%

Convected
Inward 14%

b)
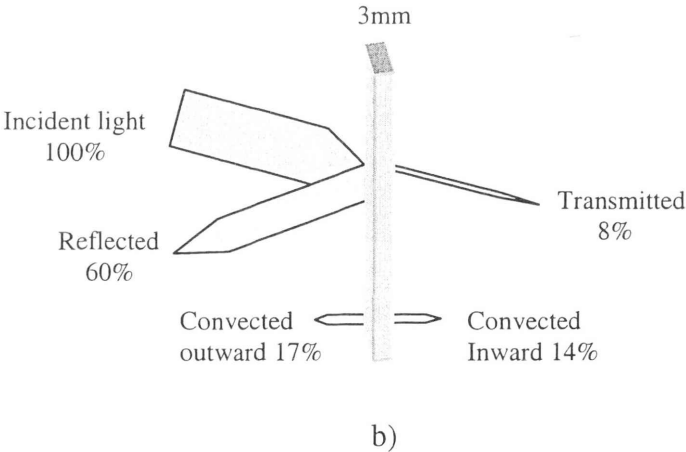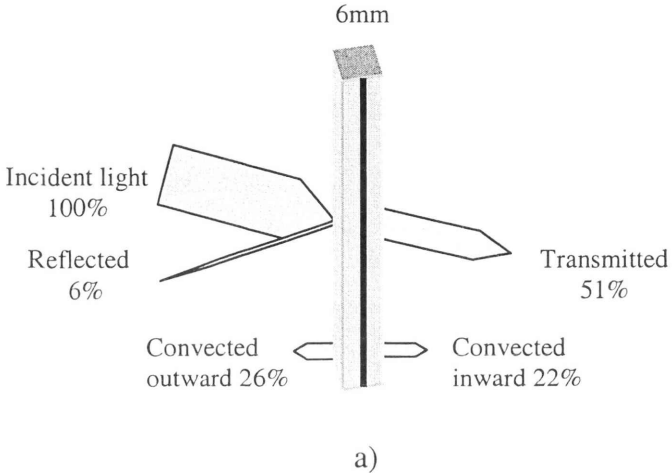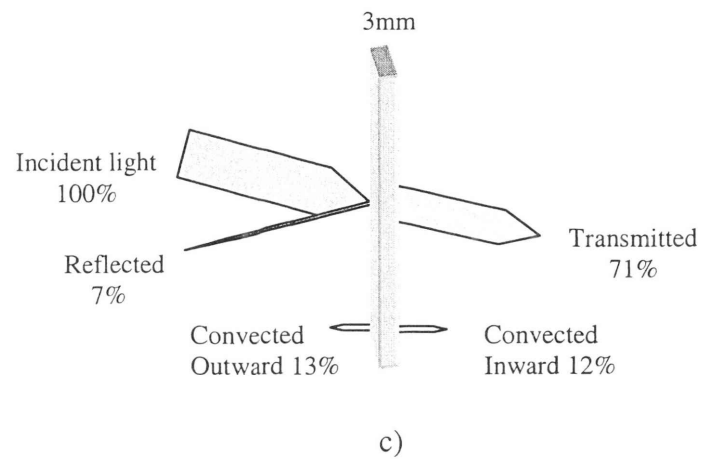
Figure 22. Energy balance for a) 6mm XL121 laminated heat absorbing glass b) 3mm $V_{kool} 40^{TM}$ heat reflective glass c) 3mm glass coated with gold nano-particles.

In conclusion, in this chapter I have verified the performance of various coated glasses in terms of their ability to block infra red, and have ranked them in the order of merit. It has been shown and confirmed that some of these special solar glazings are commercially suitable for hot climate while others are suitable for cold climate.

In the next chapter I will use this information to consider the problem of breakage in solar glazing.

CHAPTER V - Thermal stresses in window glass

5.1. Introduction

A factor that can lead to the breakage of window glass in a building is thermal stress. Thermally induced stresses in glass are caused by a temperature difference between the centre and edge of the glass. Uneven heating of the glass surface causes induction of thermal gradients in the glass resulting in thermal breakage. The uneven heating can be caused by solar irradiance or other heating sources; by natural and forced convection from wind, and air from air conditioning systems etc; and by conduction from contact with framing and other materials. A piece of glass $1.27 \times 2.54 m^2$, when heated from 0 to $38C^0$, will expand to $1.2706 \times 2.54124 m^2$ [30]. Early design consideration regarding the use of glass on commercial projects includes evaluation of potential thermal stress breakage. Performing a thermal stress analysis will allow architects and design professionals to specify the appropriate glass to ensure that the glass performs well under the expected service conditions.

The purpose of this part of the thesis is to provide:

- An overview and perspective on thermal stress in glass
- A determination of Thermal Stress Factor and Probability of Breakage (POB)
- Thermal stress analysis and calculations of failure probability.

5.2. Structural behaviour of the glass

5.2.1. Basic crystalline structure of the glass

The structure of glass is based on the silicon-oxygen tetrahedron bond (Si-O-Si bond). The tetrahedra in the Fig. 23 [31] represent three oxygen atoms clustered around one silicon atom. Theoretical strength of the glass is dictated by the molecular cohesion of

Si-O-Si bond. If for any reason the silico-oxygen tetrahedron bond is broken, a local stress is developed which can leads to the breakage of the glass.

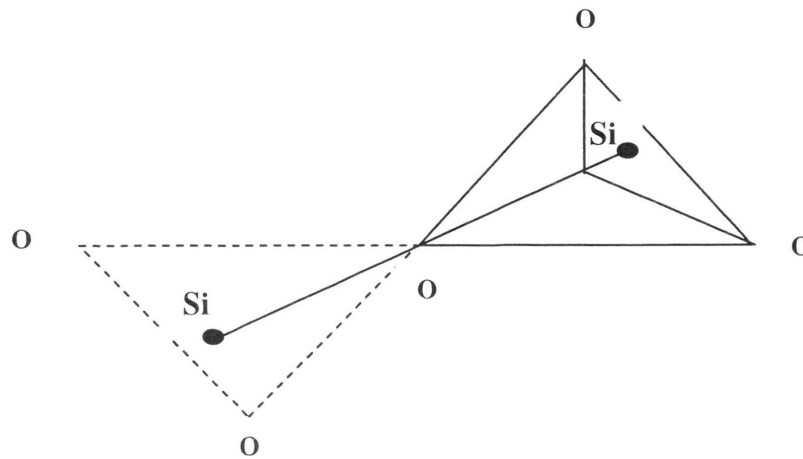Figure 23. Silicon-oxygen tetrahedron bond [31]

5.2.2. Strain on the glass

Thermal stress on glass can leads to tensile strain, compressive strain, shear strain and volumetric strain.
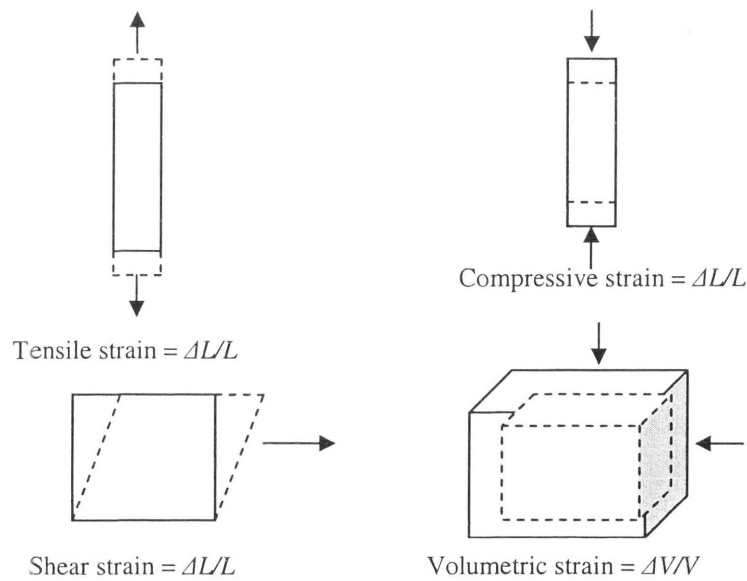

Tensile strain = $\Delta L/L$

Compressive strain = $\Delta L/L$

Shear strain = $\Delta L/L$

Volumetric strain = $\Delta V/V$

Figure 24. Schematic of various strains, showing change in length, shape or volume [31].

42

In Fig. 24 ΔL is the increase or decrease in length and L is the original length. ΔV is the decrease in volume while V is the original volume of the block.

Tensile stresses can be developed along the edge of the glass induced by the thermal gradients when it is held in a window frame. The magnitude of the edge tensile stresses depends on the solar properties of the glass, solar irradiance, glass perimeter and glazing system.

When a material behaves elastically, the stress is proportional to strain (Hook's Law). The ratio of stress over strain is a measure of elasticity.

For timescales of days and years, glass at room temperature can be considered to be an elastic material with a Young Modulus which does not very by more than ~1GPa/100K [32, 33]. When a glass specimen is strained by an applied force, it returns to its original size and shape provided the temperature is not too high, the force is not too great and the duration is short.

5.3. Thermal Expansion Co-efficient

The coefficient of linear thermal expansion is the ratio of the change in length per degree kelvin to the length at *273 K* [34]. Although the value of the coefficient is strictly speaking temperature dependent, it may be taken as a constant to a first approximation.

If l_0 is the length at 273 K, and α is the coefficient of linear thermal expansion, then the length at temperature T is given by:

$$l_t = l_0(1 + \alpha T) \tag{19}$$
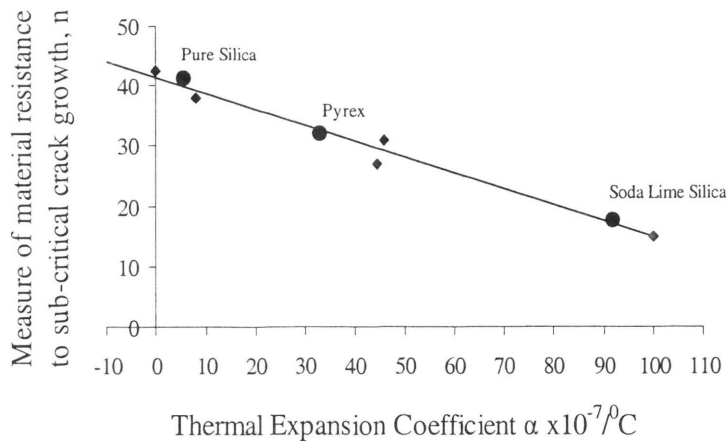
Figure 25. Thermal Expansion Coefficient for different glass substrates [31]

The thermal expansion graph as a function of material resistance in the Fig. 25 can be used to determine the expansion coefficient of various glass materials for stress analysis.

5.4. Estimation of thermally induced stress

Estimation of thermal stress on glass can be done on the basis of total solar absorbance of the glass and its thermal stress factor (TSF). Thermal Stress Factor is determined as the ratio between the nominal edge stress and solar load [35]. Solar load can be found by multiplying the maximum solar radiation incident on the surface of the glass by the total solar absorbance of the glass as a fraction.

The magnitude of the nominal edge stress can be expressed as:

$$\sigma_{thermal} = TSF \; x \; SL \tag{20}$$

Where $\sigma_{thermal}$ is expressed in kPA, TSF is the Thermal Stress Factor expressed in $kPa/(W/m^2)$, and SL is the solar load.

Thermal Stress Factor (TSF) can be obtained from a chart (Fig.26) which has been developed for three different support conditions for 6mm rectangular annealed glass [35].

Figure 26. Thermal Stress Factor chart redrawn from "A method of evaluation for thermal stress in monolithic annealed glass", by Lingnell AW and Beason L in the 2003 Glass Processing Days Conference Proceedings in Finland [35]

In Fig, 26, width of the glass perimeter strip mentioned as 'edge bite' is inserted inside the supporting frame. The 'heat sink' condition occurs when the edge bite is encased in concrete or in a thick-walled metal frame having large thermal mass. This prevents the edge of the glass from warming when the main body of the glass is exposed to solar radiation. In such a situation the central surface exposed to solar radiation rapidly reaches a higher temperature while the edge regions of the glass remain at its overnight equilibrium cool temperature. Since the edges do not expand because they remain at a particular, low temperature and the remainder of the glass expands due to an increase in temperature, the edges are in tension.

The other condition is when the glass edge is set in a thin-walled aluminium frame supported by rubber perimeter gaskets on the interior and exterior surfaces. This is called the 'conventional' condition. The glass is set in the block with sufficient clearances between glass edge and metal so that a reasonable thermal expansion can be accommodated without the introduction of support induced stress. This condition is suitable for typical wooden or vinyl window frames [35].

45

I considered the case of a door-shaped glass panel made of the 'XL121' heat absorbing glass, 0.91m by 2.53m in size to evaluate the thermally-induced edge stress in it. This shape was chosen after receiving advice from the industry. The glass panel was subjected to 500 W/m^2 of solar radiation. The panel was considered to be continuously supported on all four sides with a 6 mm edge bite, within a frame of the 'heat sink' type (Fig. 26). Since about 48% of heat flux is absorbed by the above type of glass (Table 1) the solar load (SL) out of 500 W/m^2 would be 240 W/m^2, and the thermal stress factor (TSF) would be equal to 32 W/m^2 (Fig. 26), the thermally induced edge stress then would be:

$\sigma_{thermal} = 32 \times 240 = 7.7$ MPa ≈ 8 MPa.

The stress estimated above can be compared to an allowable thermal edge stress associated with an acceptable probability of breakage using a Probability-of-Breakage Chart Fig. 27 [35].
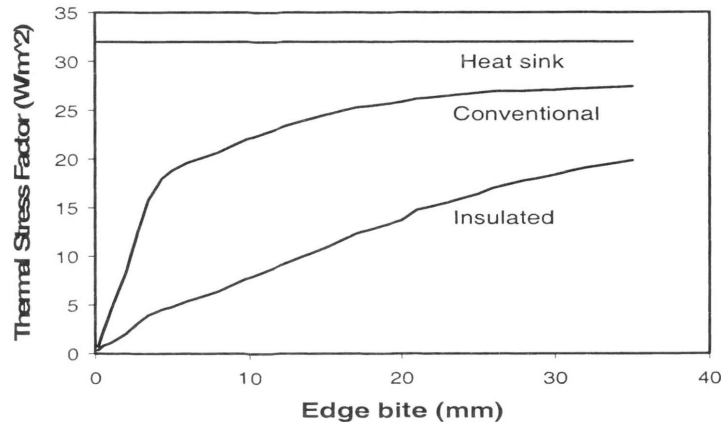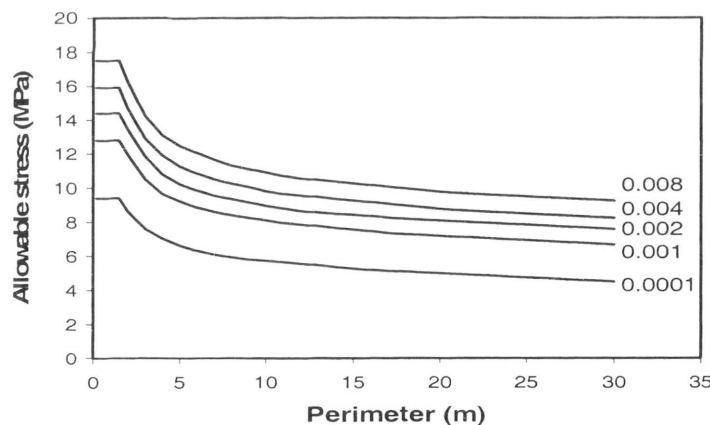

Figure 27. Probability of Breakage chart redrawn from "A method of evaluation for thermal stress in monolithic annealed glass", by Lingnell AW and Beason L in the 2003 Glass Processing Days Conference Proceedings in Finland [35]

It can be seen in the Fig. 27 that, for an edge perimeter of 6.88 m (corresponding to the door) and for a POB of 0.008, the maximum allowable edge stress is 12.0 MPa, while

for a POB of 0.0001 it is 6.3 MPa. But the stress in the glass type XL121 has been estimated as ~8 MPa. Therefore, there appears to be close to a 0.0001 probability-of-breakage per day.

5.5. Fracture Mechanics

5.5.1. Fast fracture and crack development
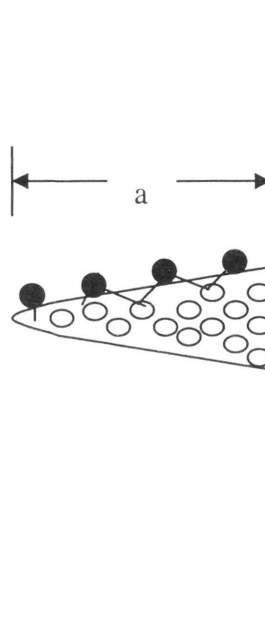
Figure 28. Crack propagation in the glass substrate [31]

Fast fracture is a term given to a phenomenon in which a flaw (such as a crack) in a material expands quickly, and causes catastrophic failure of the material [31].

It can be seen in the Fig. 28 that the silico-oxygen tetrahedron bond is broken, and a local stress concentration is developed which can lead to the breakage of the glass.

47

Critical combination of stress and crack length at which fast fracture commences is a material constant [32]. For a sheet with an edge crack

$$K_c = 1.1\sigma\sqrt{\pi a} \qquad (21)$$

Where, K_c is the fracture toughness, i e resistance to growth or propagation of surface flow. (K_c for the glass is equal to 0.7 MPa.m$^{1/2}$), σ is the allowable stress in MPa and a is the crack length in metres.

When a crack reaches some critical size a due to the stress σ applied to a material, a fast fracture will occur [31].

The risk of breakage depends on several variables, including stress, edge strength, area under stress, and time duration of the stress [36].
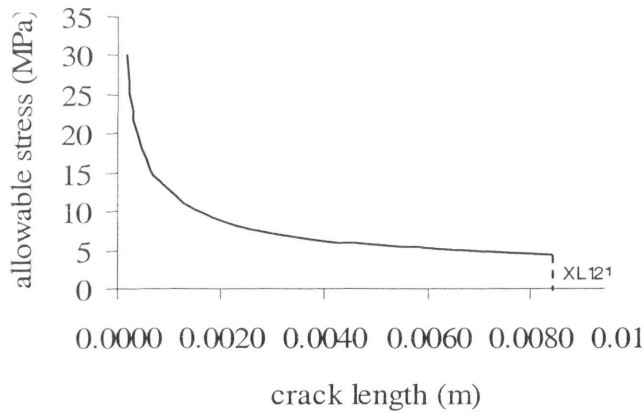
Figure 29. Crack propagation in glass length as a function of applied stress [31]

For example; stress in the glass XL121 has been estimated as 8MPa. Therefore, the size of the crack propagated in the XL121 type glass under the applied intensity would be:

$$a = \frac{k_c^2}{(1.1)^2 * \sigma^2 * \pi} = \frac{0.7^2}{1.21 * 8^2 * \pi} = 0.002m$$

It can be seen from the Fig. 29, the critical crack length of the experimental glass type XL121 under calculated stress of 8MPa is 0.002m.

5.5.2. Crack velocity
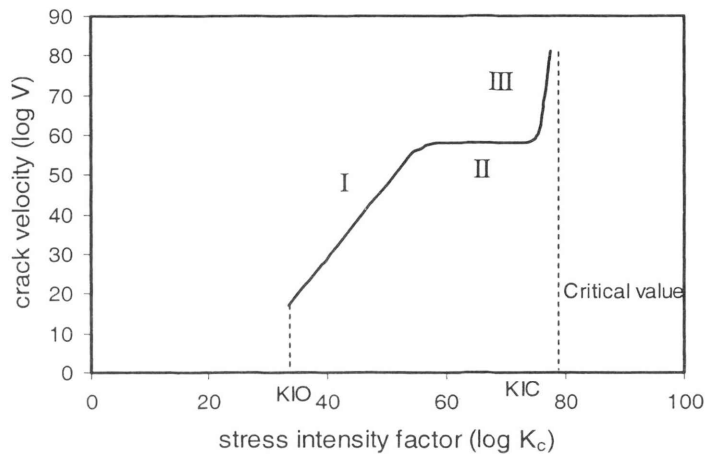
Figure 30. Crack velocity versus stress intensity factor [31]

In the Fig.30, stage *I* represents a subcritical state where the velocity of crack propagation increases slowly with the change of applied stress and *II* represents a state when the velocity is almost constant, and *III* is the situation where rapid fracture occurs with the crack velocity four times the velocity of original propagation [31].

Figure 31. Cracking observed in laminated glass door of XL121 that included an absorptive solar film in its structure.

An explanation of how a thermal breakage occurs on a clear cold winter day is as follows:

At night the glass uniformly cools to an equilibrium condition. In the morning when the sunlight begins to fall on the glass it begins to expand as the exposed area of the glass is heated. On the other hand the edges of the glass are still cold. Thus, the unheated edges of the glass around the perimeter experience a tensile stress parallel to the edge of the glass. If this thermally induced stress exceeds the edge strength of the glass, breakage will occur (Fig. 31). Glass edge strength is reduced by any damage that occurred during handling, fabrication and installation. Fracture originates from this damage.

5.5.3. Factors influencing the glass thermal stress

Glass thermal stresses are influenced by a number of product and environmental factors. The most significant contributors to thermal stresses are [37]:

- Glass type
- Coating type and coating location
- Exterior shading patterns
- Interior solar control devices
- Heating appliance location and orientation

The temperature gradients that cause thermal stress typically arise when the sun heats an exposed area of cool glass. The speed and the amount of the temperature increase are directly related to the absorbency of the glass.

Outdoor shading patterns can be caused by any combination of design features, such as overhangs, fins and curtain wall members as well as elements of surrounding environment including adjacent buildings and trees. The effect of these patterns on thermal stresses depends on the type of pattern and percentage of glass area shaded. Generally, shading patterns with 50% or less coverage of glass area are more dangerous because they cause the higher temperature gradients. Shading patterns vary due to

changes in incident angle of solar radiation and significant ambient temperature variations during the spring and autumn.

Indoor shading devices increase the temperature of the central area of the glass in two ways because they:

- Reflect solar radiation back through the glass
- Decrease convection and conduction of heat through the glass to the outdoors

The effect of an indoor shading device is dependent on the type and color of device used, and the amount of ventilation that exists within the air space between the shading device and the glass. Ventilating the air space will help to reduce edge stress.

Thermal breakage can also occur due to heating appliances, which direct warm air against cold glass. The trapped heat that comes from heating appliances located between the interior shading device and the glass can cause the center of the glass to become excessively warm and lead to glass breakage.

In conclusion, in this chapter I have presented methods by which thermally induced stress and probability of fracture in glass can be estimated. However, in the next Chapter I will show how the stress state in the glass can be more accurately estimated using Finite Element Analysis. In this exercise I considered three types of glass: clear glass, tinted glass, and glass coated with gold nano particulates.

CHAPTER VI - Finite element analysis

6.1. Introduction

As explained in the previous chapter various coatings and tints applied to window glass have the ability to reflect or absorb infrared radiation incident from the sun and thereby reduce heat load in the interior of a building. However, in the case of glass coated with absorptive materials, the surface becomes hot as a result. This increased glass temperature causes thermal expansion, which if uneven or if not matched by expansion of the window frame, will cause stresses within the pane. In most circumstances the edge of the glass is subjected to higher tensile stresses than its surfaces so if thermally-induced stress exceeds the edge strength of the glass, breakage will occur. Reports of coated glass panes that had unexpectedly fractured during service prompted me to investigate the magnitude of the thermal stresses developed in glass coated with infrared absorbing materials, and the relationship of these stresses to uneven illumination by sunlight. The stresses in two simplified geometries were modelled using Finite Element Analysis (FEA). These calculations were not intended to quantitatively replicate the stresses in any real window, but were rather carried out in order to qualitatively illustrate the phenomena and determine the order of magnitude of the stresses that occur in coated glass panes subjected to solar illumination.

A particular case study was made of the thermally-induced stress in a door-shaped glass pane measuring 0.91 by 2.53 m and subjected to partial solar illumination. This was selected after discussions with an industrial contractor, who provided an example of such a structure that had cracked, Fig.31, when it had been illuminated by morning sunlight. 'XL121' was the material used in the glass panel illustrated in Fig.31. The solar screening functionality of glass pane had been achieved by means of a polymer film containing a substance that preferentially absorbed infrared radiation. The rise in temperature of the glass causes expansion, and under some circumstances as I will show here, stresses concentrations at critical locations.

The finite element package used was 'Ansys' by Ansys Incorporated, of USA. A user-defined rate of heat generation was imposed on the lower half of the glass panel. A two dimensional model under steady state condition was considered for the thermal part of the analysis, and 'Quad 4node 55 (PLANE55)' element was chosen in Ansys. Only the steady-state thermal and load solutions were considered. It was assumed that rapid equilibration of temperature occurred in the through thickness direction so no variation of temperature in the through thickness was assumed. Because of the dependency of glass elastic modulus and other physical properties on temperature [39] the behaviour of the glass would be slightly non-linear. However, I have adopted a linear elastic approach since the state of stress in this elastic system is dominated by the value of Youngs modulus, which does not vary by more than ~1GPa/100K [33], giving a variation of only 0.4% over the temperature range (20 to 50°C) of interest, using the material properties at 20°C as input parameters. The values for material parameters [27, 40], Table 3, and estimates for the heat transfer coefficient, h, defined by using Eqs. (11), (12), and (13) were implemented as a requirements of the FEA.

Table 3. Material properties used for basic 3 mm of soda-lime glass [27, 40].

Properties	Symbol	Value	Units
Thermal expansion co-efficient	α	90×10^{-7}	/°C
Modulus of elasticity (Young Modulus}	E	6.3×10^{10}	Pa
Poisson's ratio	υ	0.22	
Emissivity	ε	0.92	
Density	ρ	2500	kg/m^3
Thermal conductivity	k	1.4	W/m.K
Specific heat	c_p	750	J/kg.K
Front face temperature (measured)	T_f	312	K
Back face temperature (measured)	T_b	310	K
Heat transfer co-efficient at front face (calculated)	h_f	4.6	W/m^2
Heat transfer co-efficient at back face (calculated)	h_b	4.4	W/m^2

Finally, the actual FEA itself was carried out in two steps. First, the meshed model was created, the preference set to 'thermal', the heat transfer problem solved, and the results saved to disk. Next the heat transfer boundary conditions and thermal loads were

removed from the mesh, the preference changed to 'structural', the element type switched from 'thermal' to 'structural', the calculated temperature distribution re-imposed, and the displacements due to the calculated temperatures applied.

6.2. Results

6.2.1. The determination of surface temperature

The rise of the surface temperature of the glass due to the presence of the absorptive coating leads to convective heat transfer to the external and internal environments, Eq. (8). The relative proportions of heat convected inwards or outwards depend on the air temperatures and velocities in internal and external environments must be taken into account. As mentioned previously a small proportion of the absorbed energy is re-emitted as radiation but this effect is small for the low values of T and ΔT involved.

Various surface temperatures (T_s) may be assumed in Eq. (10), and used to give corresponding values of h using Eq. (11) to Eq. (13). Finally, the total heat convected from front and back surfaces can then be calculated, which will be equal to the total heat absorbed by the glass pane (Fig.32). The resulting graph can be used to determine the actual amount of heat absorbed by a surface when its surface temperature is known and vice versa.
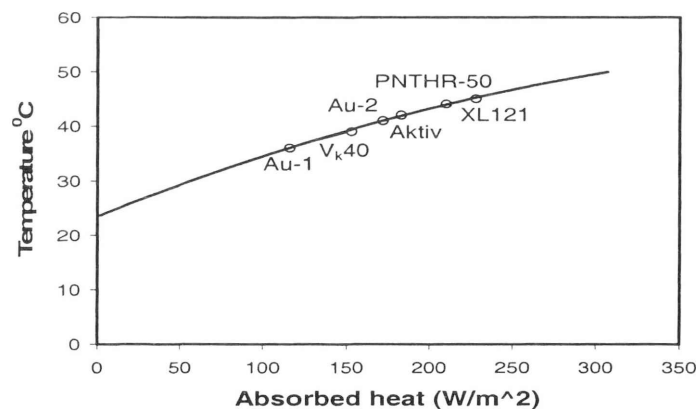

Fig. 32. Temperature of the glass surface as a function of absorbed heat showing surface temperatures of various experimental glazing systems, under a flux of 500 W/m^2 of tungsten lamp illumination.

The temperature of the glass is determined by the air speed and convective conditions and the quantity of heat absorbed, not directly by the insolation.

6.2.2. Case study: door-shaped glass panel

The glass door was modelled with its bottom half in full sunlight and its top half at an initial temperature of 293K (20°C), The heat load was applied to the bottom half of the door, and the top and bottom edges of the door were considered to be infinite heat sinks at 293K. The imposed heat load was systematically varied between 0 W/m^2 and 300 W/m^2 in order to provide data for a wide range of absorptive glass types. Two different structural scenarios were considered. In the first the door was fixed at the top and bottom to an infinitely stiff structure at 293K, and in the second only the bottom edge was pinned.

In the first case, the thermal expansion of the heated glass generated significant compressive stresses in the y direction, Fig 33(b). It can be observed from Fig. 33(b) that compressive stresses developed at the corner of the door are significantly higher than that developed in the middle due to rigidly fixing the top and bottom of the glass door.
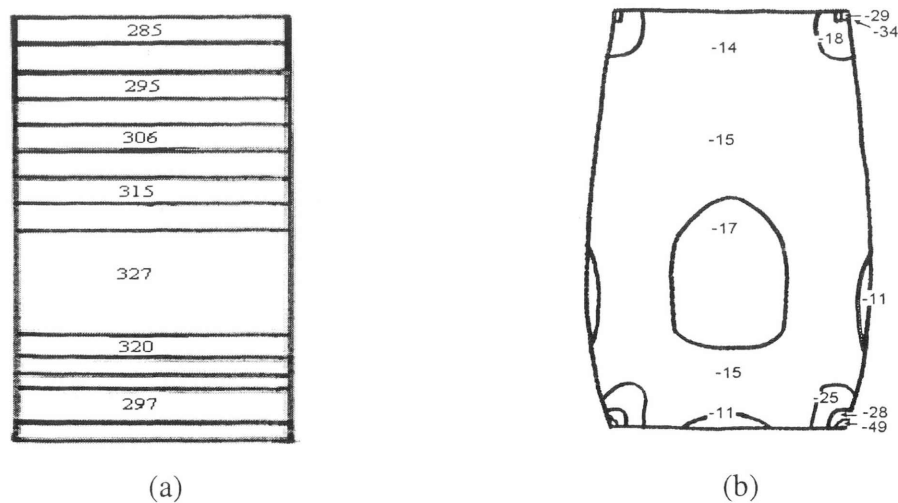

(a)   (b)

Fig. 33. a) Temperature distribution in Kelvin scale, b) Contour diagram showing σ$_y$ developed in glass door subjected to illumination at 200W/m^2 on its lower half, while being rigidly fixed top and bottom to an infinitely stiff support.

There is not much variation of the stresses developed around the mid surface of the glass door. However, besides some possible buckling, this situation is not likely to cause failure since edge defects in the glass will not propagate under compressive loads. Maximum compressive stresses developed in the centre of the door due to various imposed heat loads at its lower half were analysed. It can be seen from the Fig. 34 that compressive stress increases proportionally as the load increase.
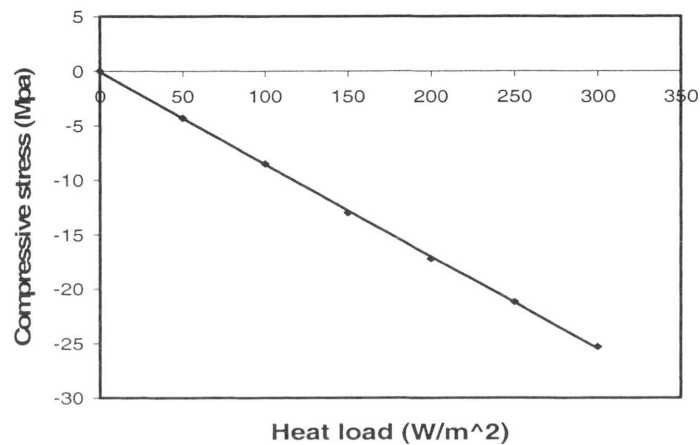

Figure. 34. Maximum compressive stress developed in centre of glass door set at top and bottom into a rigid support, as a function of heat load.

In contrast, significant tensile stresses are generated in the second scenario, where the glass door is fixed only at its base. Fig. 35 shows the principal stresses, σ_1, calculated for a heat load of 200 W/m^2, as an example. There is a concentration of tensile stress along the flanks of the glass at position A, and along the base. While the tensile stress σ_1 at position A is oriented in the y-direction, and will therefore tend to cause breakage, the maximum in stress σ_x, along the base is actually at position B. This is because the principle stress σ_1, elsewhere along the bottom edge is rotated out of the x-direction, with a resulting x-component less than that of σ_x at B. The variation in σ_y at position A, and σ_x at position B, is plotted as a function of heat load in Fig. 36. It is evident that tensile stresses of up to 7 MPa can act along the edges of the glass under the assumed conditions.

56
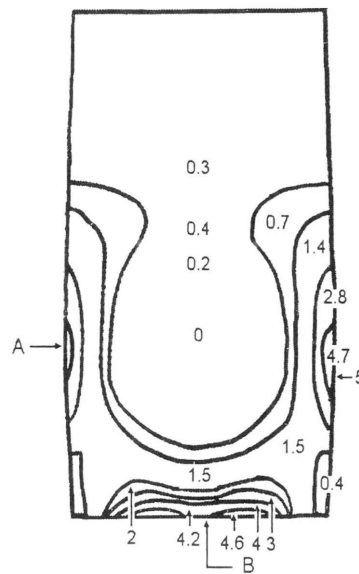
Figure. 35. Contour diagram showing principal stress σ_1 developed in the glass door when subjected to illumination at $200W/m^2$ on its lower half, while being rigidly fixed only along its lower edge.

Figure. 36. Maximum tensile stresses developed along edges of glass door fixed only at its base, as a function of heat load.

The induced stress in the XL121 glazing has been estimated as ~8 MPa and ~6 MPa by FEA (at position A, Fig. 36). Therefore, there appears to be close to a 0.0001

57

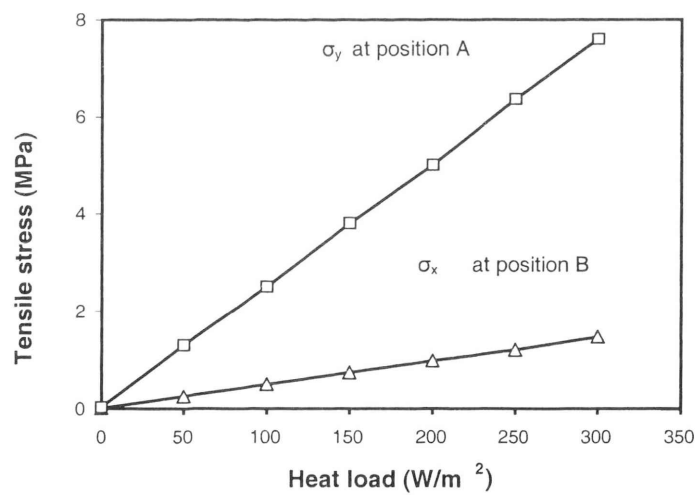probability-of-breakage per day (Fig. 27). This alone might be cause for concern, but it should be further noted that any stress concentration induced by faulty installation will further exacerbate the problem.

In an alternate approach to the problem, fracture mechanics can be invoked to provide some insight into the problem of breakage. The critical combination of stress and crack length at which fast fracture commences is given for an edge crack as Eq.(21).

The net effect of Eq. (21) is to impose a maximum safe stress for any given crack size, please see Fig. 37. I concede that Eq. (21) is derived for an infinitely sharp crack in perfectly elastic solid, but will conservatively assume here that because glass is so brittle, it can be applied to any defect of length.
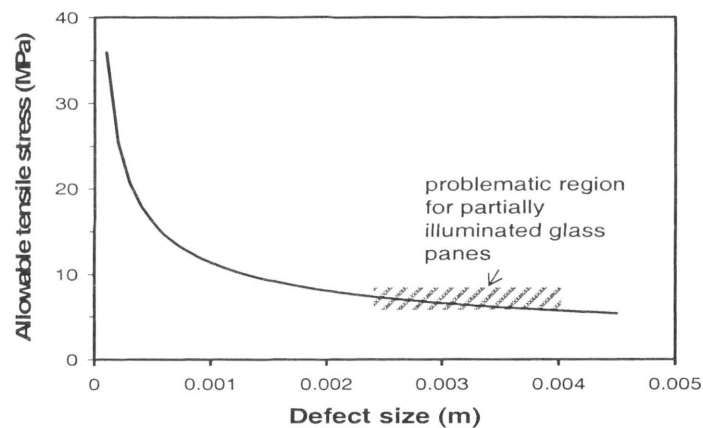

Figure 37. Maximum allowable stress as a function of crack size in glass.

It is evident that under the conditions of the test explored here maximum tensile edge stresses in the range of 6 to 8 MPa are likely in the glass door. Analysis shows that the maximum edge flaw that can be tolerated in these glass doors is of the order of 2 to 3.5 mm. While the glass is likely to be shipped from the wholesaler in good condition, it is possible that a defect of these dimensions can arise due to cutting, or to chipping during handling.

In conclusion, the thermal stress developed in partially illuminated panes of heat absorbing glass was investigated. Temperature and stress distributions in a simplified,

illustrative configuration were calculated with the assistance of finite element analysis. The aim of the analysis was to gain a better understanding of the response of glazed structures under radiative thermal loads. Edge stresses of ~6 to 8 MPa can be readily generated in heat absorbing glass under some conditions of constraint and illumination. These stresses are sufficient to raise the probability of failure of a glass door to 0.0001. Application of a simplified fracture mechanics principle reveals that defects of no larger than 2 or 3 mm could be tolerated under these conditions.

CHAPTER VII - Conclusions

Reflection and absorption are the two competing strategies for attenuating solar radiation transmitted through windows. In general, coatings of certain dielectric compounds absorb light while metallic coatings reflect it. It was observed that the V_{Kool} multi-layered sputter coated film on 3 mm glass is simultaneously both strongly reflective and absorptive. The XL121 and PNTHR50 systems, in contrast, are basically just strong absorbers.

The two experimental glass panes coated with gold nano-particles at UTS by fellow student Mr X. Xu had rejected 21 and 25% of heat and possessed a relatively light tint. Though conventional gold-coated glass is a reflector of radiation, these two coated glasses basically appeared to be absorbers. This changed mechanism is due their novel microstructure. The layer of hemispherical gold nano-particles of this coating exhibit a plasmon resonance at low concentration with the incoming light, with the effect dependent on density and morphology of the particles. In the present work the light was attenuated due to this resonance with wavelengths in the region of 600 to 700 nm, with the absorbed energy manifesting as heat. However, it has been shown that the percentage of light reflected from coatings of gold nanoparticles increases as the density of the coatings increase [21].

Thermal breakage is generally recognised to start perpendicular to the edge of the glass and result in a 'meandering' crack. Factors that influence thermal stresses on the glass surfaces have been investigated in the current project. Finite element calculations of temperature and stress have been conducted. The aim of the analysis was to gain a better understanding of response of the glazing systems under the thermal loads. It was observed that stress values and deformation for all of the experimental glazings under the imposed thermal loads and with applied boundary conditions were lower than the maximum allowable stresses according to the Probability of Breakage Chart (Fig. 27).

References

[1].   http://www.londoncrownglass.co.uk/History.html. Accessed on 1st July 2004 at 2pm.

[2].   Garden GK (1964). "Characteristics of window glass". *Canadian Building Digest-CBD-60;* IRC, Canada.

[3].   Dai Y (2001). "Solar control film retrofitted energy efficient windows for tropical climate". *Glass Processing Days Conference Proceedings 2001;* Tamglass Ltd. Tampere, Finland, pp 156-161.

[4].   ASTM G 159 – 98 (1998). "Standard tables for references solar spectral irradiance at air mass 1.5: Direct normal and hemispherical for a 37° tilted surface". *American Society for Testing and Materials;* West Conshohocken, PA, USA.

[5].   ASTM E971-88 (Reapproved 2003). "Standard practice for calculation of photometric transmittance and reflectance of materials to solar radiation". *ASTM International;* 100 Barr Harbor Drive, PO Box C700, West Conshohocken, PA 19428-2959, United States.

[6].   Bell JM and Matthews JP (1998). "Glazing materials". *Materials Forum;* 22, pp 1-24.

[7].   http://www.eere.energy.gov/erec/factsheets/eewindows.html. Accessed on 1st July 2004 at 4pm.

[8].   Nadel SJ and Hill RJ (1997). "Durable low-e coated glass for use in warm temperate climates". *Glass Processing Days Conference Proceedings 1997;* Tamglass Ltd. Tampere, Finland, pp 209-212.

[9]. Takeda H, Yabuki K and Adachi K (2001). "Coating solution for forming a film for cutting off solar radiation and the film formed there from". *United States Patent;* 6319613, USA.

[10]. Smith GB, Deller CA, Swift PD, Gentle A, Garrett PD and Fisher WK (2002). "Nanoparticle-doped polymer foils for use in solar control glazing". *Journal of Nanoparticle Research;* 4, Kluwer Academic Publishers, Netherlands, pp 157-165.

[11]. http://www.eng.fsu.edu/~alvi/EML4304L/webpage/experiment_1.htm. Accessed on 24th March 2003 at 3pm.

[12]. Krc J, Zeman M, Kluth O, Smole F, and Topic M (2002). "Experimental investigation and modelling of light scattering in a Si:H solar cells deposited on glass/ZnO:Al substrates". *Material Research Society;* vol 715, Julich, Germany.

[13]. Foley JD, van Dam A, Feiner SK and Hughes JF (1990). "Computer graphics. principles and practice". *The Systems Programming Series;* 2nd Edition, Chapter 13, Addison-Wesley, Reading, Massachusetts, USA.

[14]. *http://irc.nrc-cnrc.gc.ca/cbd/cbd052e.html.* Accessed on 31st March 2004 at 1pm.

[15]. *http://www.ppg.com/gls_residential/share/hom_hot.htm.* Accessed on 22nd March 2003 at 12pm

[16]. Hofmann T and Kursawe M (2003). "Antireflective coatings on glass for solar applications". *Glass Processing Days Conference Proceedings 2003;* 8th ed. Tamglass Ltd. Tampere, Finland, pp 382-384.

[17] Huber M and Proft B (2003). "TiO_2-coatings from inorganic soles". *Glass Processing Days Conference Proceedings 2003*; 8th ed. Tamglass Ltd. Tampere, Finland, pp 328-329.

[18]. Wittkopf H (1997). "Electro-chromic for architectural glazing applications". *Glass Processing Days Conference Proceedings 1997;* Tamglass Ltd. Tampere, Finland, pp 299-303.

[19]. Fischer U, Hausler T, Rogab H, Rottmann M, Kraft A and Heckner KH (2003). "Heat transport and thermal expansion of electro-chromic glazing systems with voltage controlled transmission due to solar irradiation". *Fifteenth Symposium on Thermo-physical Properties;* Boulder, Colardo, USA.

[20]. Genzel L and Martin TP (1973). "Infrared absorption by surface phonons and surface plasmons in small crystals". *Surface Science;* 34, pp 33-49.

[21]. Ung T, Liz-Marzán LM and Mulvaney P (2002). "Gold nanoparticle thin films". *Colloids and Surfaces A: Physicochemical and Engineering Aspects;* 202, pp 119-126.

[22]. Xu X, Stevens M and Cortie MB (2004). "In situ precipitation of gold nanoparticles onto glass for potential architectural applications". *Chemistry of Materials;* vol. 16(1), pp 2259-2266.

[23]. Oldenburg SJ, Averitt RD, Westcott SL and Halas NJ (1998). "Nano engineering of optical resonances". *Chemical Physics Letters;* 288, pp 243–247.

[24]. Prodan E and Nordlander P (2003). "Structural tunability of the plasmo resonances in metallic nanoshells". *NanoLetters;* 3, pp 543-547.

[25]. Anonymous (1992). "Energy efficient window glazing systems – a pacific energy center architecture fact sheet". *PEC On-line Resource;* Pacific Gas and Electric Company, New York, pp 1-3.
http://www.pge.com/pec. Accessed on 11th January 2005 at 3 pm.

[26]. Holman JP (1992). *Heat Transfer.* Chapter 7, 7th edition, McGraw Hill, London.

[27]. Incropera FP and DeWitt DP (1996). *Fundamentals of heat transfer*. John Wiley & Sons, New York.

[28]. Anonymous (1994). "Heat storage, diversity & stratification". *Air Conditioning Systems Design Manual - Australian Department of Housing and Construction Handbook*; Chapter 3, Table 5, Australian Government Publishing Service, Canberra.

[29]. ISO 10526: (1999). "CIE standard illuminants for colorimetry". *International Organization for Standardization*; Geneva, Switzerland.

[30]. Anonymous (2002). "Thermal stress". *Technical Information*; Pilkington North America Inc. Toledo Ohio.

[31]. Gulati ST (2003). "Calculation of stresses in automotive and architectural glasses". *Glass Processing Days Conference Short Course 2003*; Tampere, Finland.

[32]. Ashby MF and Jones RH (1980). "Engineering materials-an introduction to their properties and applications". *International Series on Materials Science and Technology;* v34, Oxford, UK.

[33]. Warren PD (2004). Pilkington Glass, U.K. Private communication (written), 8th December 2004.

[34]. *http://www.glassresource.com/sub/tough/thermal.htm*. Accessed on 6th February 2004 at 11am.

[35]. Lingnell AW and Beason L (2003). "A method of evaluation for thermal stress in monolithic annealed glass". *Glass Processing Days Conference Proceedings 2003*; Tamglass Ltd. Tampere, Finland, pp 291-293.

[36]. *http://www.saint-gobain-glass.com/uk/2_7_6.htm*. Accessed on 3rd February 2004 at 10am.

[37]. Anonymous (1883). "Thermal stress update". *Glass Technical Document*; PPG Industries Inc, Pittsburgh, PA 15238 – 8361, USA, pp 1-6.

[38]. Chowdhury H, Xu X, Huynh P and Cortie MB (2004). "Radiative heat transfer across glass coated with gold nano-particles". *Journal of Solar Energy Engineering (ASME);* in press, publication due February 2005.

[39]. Anonymous (1998). "Steady state thermal analysis". *Thermal Analysis Guide;* Chapter 2, Ansys Inc, Southpointe, Canonsburg, PA 15317, USA. *mk:@MSITStore:C:\Program%20Files\Ansys%20Inc\v80\commonfiles\help\en-us\an.* Accessed on 15th December 2004 at 3 pm.

[40]. *http://www.abrisa.com/downloads/soda_lime_float.pdf.* Accessed on 21st December 2004 at 9a m.

Appendix A – Detail specifications of the sensor

PMA1143 Thermopile

Detector Specifications

Features

- flat spectral response
- portable
- hermetic enclosure
- min/max tracking
- dose integration

Applications

- Flat spectral response measurements
- Control ovens
- Reference measurements
- IR applications

The PMA1143, Thermopile is manufactured by Kipp & Zonen, the world pioneer in thermopile pyranometer manufacturing. It brings the unsurpassed features and high accuracy of this class of instruments into the price range of photovoltaic detectors.

The sensor is a high quality blackened thermopile assuring flat spectral response throughout the entire spectrum.

Specifications

Spectral response
Without window	0.2-50μm
With window	0.3-3μm

Sensitivity

homogeneous irradiance on front window approx.   20-40 μV/Wm^2
power falling through window and aperture
  stop directly on the absorber approx.   0.1 μV/μW
  without window   1.10 x higher
Response time (95%)   30 seconds
Field of view   10°
Non-linearity (50mV)   3%
Weight   0.5 Kgram

Sensitivity:

For a homogeneous irradiance on the front window = 34.0{μVplt/(W/m^2)]

For radiation falling through the window and aperture stop directly on the absorber

= 0.081 [μVolt/μWatt]

# Appendix B - Total energy received by the glass pane
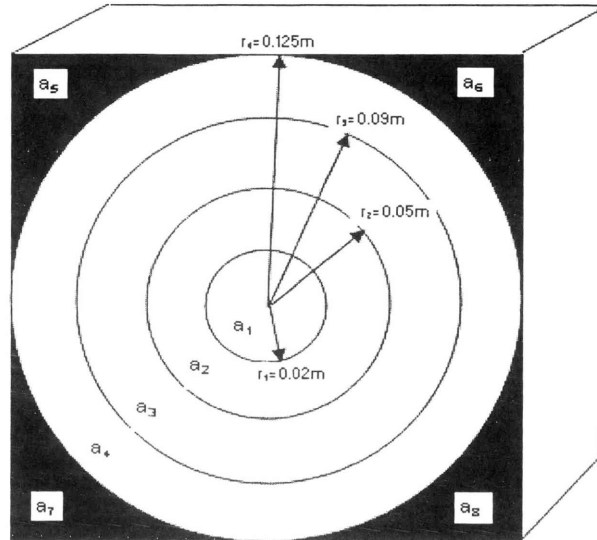
Area of the section (a)m^2	Sensor reading (x)mV	Sensor calibration factor y=500/17	Light energy fall on each section of the glass (p=a*x*y) Watts	Total light energy received by the glass (Q$_{incident}$)Watts
a$_1$ = πr$_1^2$ = 0.0013	17	29.41	0.63	
a$_2$ = πr$_2^2$-πr$_1^2$ = 0.0066	17	29.41	3.3	
a$_3$ = πr$_3^2$-πr$_2^2$ = 0.0176	16.3	29.41	8.43	**29**
a$_4$ = πr$_4^2$-πr$_3^2$ = 0.0236	16	29.41	11.12	
Area of the black spaces (a$_{5+}$a$_{6+}$a$_{7+}$a$_8$) = (0.0625) - πr$_4^2$ = 0.0134	14.7	29.41	5.81	

Appendix C - Total energy transmitted

(Example:V_{kool}40 type)

Area of the section (m^2)	Sensor calibration factor (y=500/17)	Sensor reading (x)mV	Light energy transmitted through each section (p=a*x*y) Watts	Total heat energy transmitted (Watts)
0.0013	29.41	1.4	0.05	
0.0066	29.41	1.4	0.27	
0.0176	29.41	1.3	0.67	**2.25**
0.0236	29.41	1.2	0.83	
0.0134	29.41	1.1	0.43	

Appendix D - Phong's illumination model

While n = 1

While n = 5

While n = 50

While n = 64
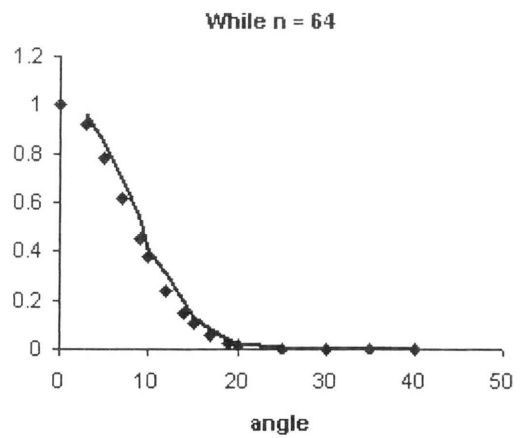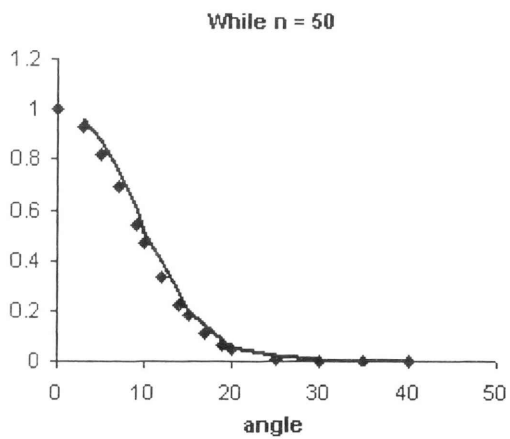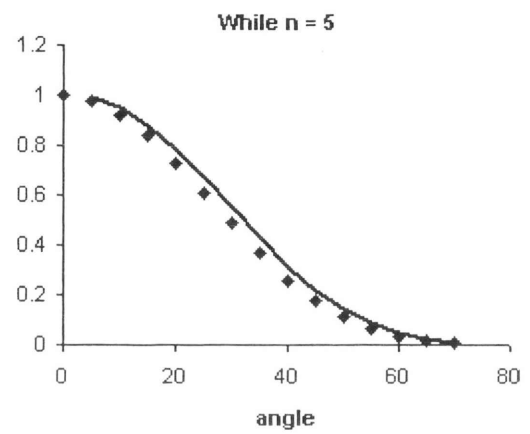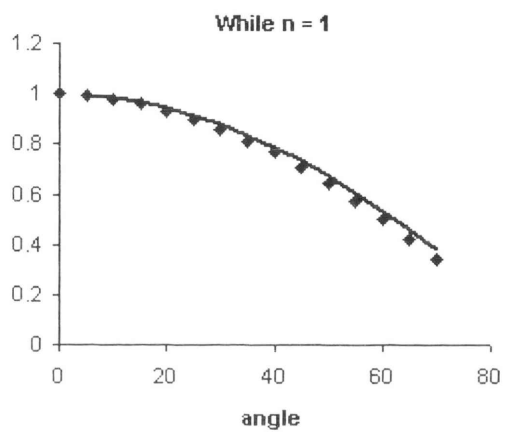
Appendix E – Determination of heat transfer coefficient *(h)* (Example: V$_{kool}$40 type)

Film temperature $T_f = \dfrac{t_s + t_a}{2}$ Where

Surface temperature $t_s = 39^o C$

Air temperature $t_a = 21^o C$

Therefore, film temperature $T_f = 30^o C$ or $= 303K$

Volumetric thermal expansion $\beta = \dfrac{1}{T_f} = \dfrac{1}{303} = 0.0033 K^{-1}$

Now properties of air taken from table A.4 [36] based on film temperature T$_f$ as below

| Kinematic viscosity υ (m^2/s)	Thermal conductivity k (W/m.K)	Volumetric thermal expansion B (K^{-1})	Prandtl number Pr	Characteristics length L (m)
1.47E-05	2.66E-02	0.0033	0.71	0.25

Grashof number $Gr_L = \dfrac{g\beta(t_s - t_a)L^3}{\upsilon^2} = 4.225E + 07$

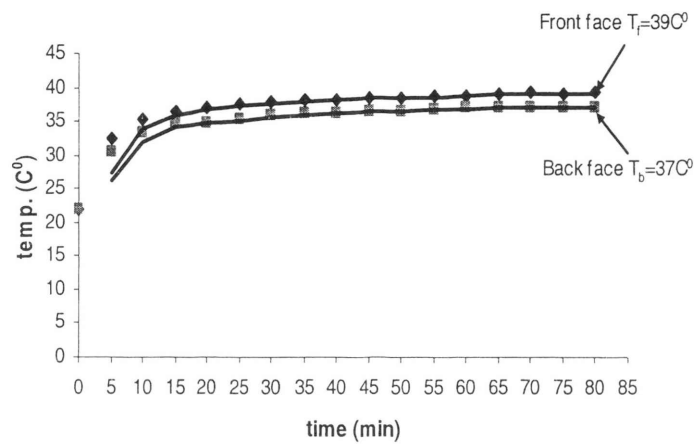Rayleigh number $Ra_L = Gr_L \times \mathrm{Pr} = 3E + 07$

Nusselt number $Nu_L = \left\{ 0.825 + \dfrac{0.387 Ra^{1/6}}{\left[1 + \left(\dfrac{0.492}{\mathrm{Pr}} \right)^{9/16} \right]^{8/27}} \right\} = 42.82$

Now heat transfer co-efficient $h = \dfrac{Nu_L k}{L} = 4.55 W / m^2$

Appendix F - Heat transfer coefficient *(h)* of various experimental glazing systems
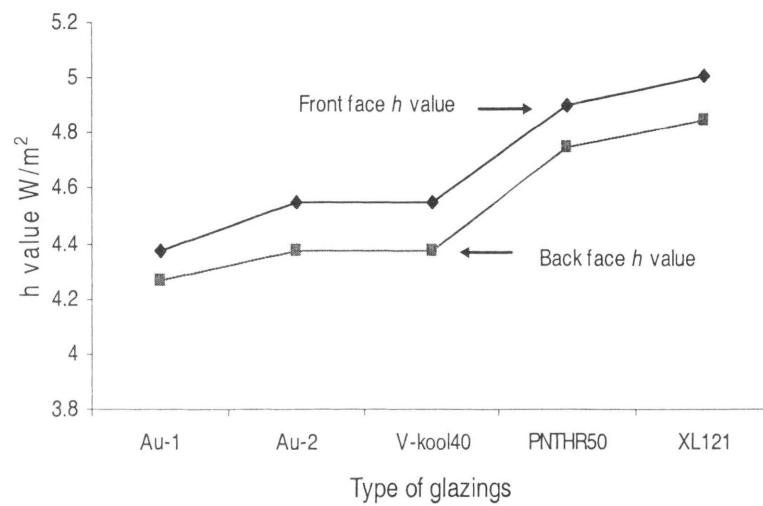
Appendix G - Energy convected from front and back faces of the glass pane (Example: $V_{kool}4o$ type)

Temperature as a function of time

$T_{ambient}$ (C^0)	Area (m^2)	h (Watts/m^2/C^0)
21	0.0625	4.55

$Q_{conv.\ front} = (T_f - T_{air})*A*h = \mathbf{4.8\ W/m^2}$	

T_{frame} (C^0)	Area (m^2)	h (Watts/m^2/C^0)
21	0.0625	4.37

$Q_{conv.\ back} = (T_f - T_{air})*A*h = \mathbf{4.1\ W/m^2}$

Where h is the calculated heat transfer co-efficient in Watts/m^2/C^0 (see appendix G) and A is the area of the glass in m^2

72